Geochemistry, Geophysics, Geosystems®

AGU ADVANCING EARTH AND SPACE SCIENCE

RESEARCH ARTICLE
10.1029/2021GC010300

Special Section:
Phanerozoic Tectonics and Volcanism in the Arctic

Stratigraphic and Spatial Extent of HALIP Magmatism in Central Spitsbergen

Kim Senger[1] **and Olivier Galland**[2]

[1]Department of Arctic Geology, The University Centre in Svalbard, Longyearbyen, Norway, [2]Department of Geosciences, NJORD Centre, University of Oslo, Oslo, Norway

Key Points:

- Igneous intrusions are well exposed in central Spitsbergen across a range of host rocks
- Two-hundred sixty five intrusions cover 72 km^2 of the onshore part, and a further 3,000 km^2 of intrusions are characterized by geophysical data
- Igneous intrusions and associated aureoles are characterized by wireline data

Correspondence to:
K. Senger,
kim.senger@unis.no

Citation:
Senger, K., & Galland, O. (2022). Stratigraphic and spatial extent of HALIP magmatism in central Spitsbergen. *Geochemistry, Geophysics, Geosystems*, *23*, e2021GC010300. https://doi.org/10.1029/2021GC010300

Received 1 FEB 2022
Accepted 4 NOV 2022

Author Contributions:
Conceptualization: Kim Senger
Data curation: Kim Senger
Formal analysis: Kim Senger
Funding acquisition: Kim Senger
Methodology: Kim Senger
Resources: Kim Senger
Software: Kim Senger
Validation: Kim Senger
Writing – original draft: Kim Senger

Abstract Rapid extensive magmatism may have a profound effect on global climate by liberating and releasing greenhouse gases to the atmosphere through contact metamorphism of lithologically heterogeneous host rocks and degassing of magma and associated lava flows. The high Arctic Archipelago of Svalbard offers accessible, superbly exposed outcrops revealing Early Cretaceous magmatism associated with the High Arctic Large Igneous Province (HALIP). In this contribution, we investigate the onshore-offshore intrusive complex of central Spitsbergen formed due to HALIP activity, that is, the Diabasodden Suite. This is the most "data-rich" part of Svalbard due to past petroleum exploration and research drilling. In this area, the predominantly dolerite intrusions are emplaced in a range of host rocks ranging from Permian carbonate-dominated successions to organic-rich shale-dominated successions of Middle Triassic and Late Jurassic-Early Cretaceous age. Two hundred sixty five individual igneous intrusions, covering 72 km^2, are exposed onshore in the study area. This equates to approximately 0.14–2.5 km^3 of emplaced magma. In addition, subsurface characterization using borehole, seismic and magnetic data indicates that an area of additional ca. 3,000 km^2 is affected by magmatism (magma volume 3.2–195.2 km^3). Wireline logs in boreholes characterize both intrusions and associated aureoles. Aureoles with very low resistivity indicate occurrence of organic-rich shales suggesting past fluid circulation and de-gassing. This study forms the foundation for quantifying HALIP-related magmatism in the data-poorer parts of Svalbard, and other circum-Arctic basins.

Plain Language Summary Volcanic eruptions are known to influence global climate today. In the past, even greater volcanic eruptions have happened than we know today, and some of these likely caused major global climatic shifts and contributed to mass extinctions. Volcanic eruptions are fed by a complex of sub-surface magma pathways. If magma in such "plumbing systems" does not reach the Earth's surface, it will solidify horizontally (as sills) or vertically (as dykes). Together dykes and sills form an igneous complex that heats up the surrounding rocks and may cause the release of gas during this process. If this happens relatively near to the surface, this gas may escape to the atmosphere and contribute to global climate change. The key variables that control the extent of climate effects include the emplacement depth, the spatial extent of the magmatism and the lithology of the host rocks. In this paper, we examine the igneous complex of dykes and sills in Spitsbergen in the high Arctic. We use borehole, seismic and field data to calculate how much magma was emplaced in this area and discuss whether it may have contributed to global climate change approximately 125 million years ago.

1. Introduction

The high Arctic experienced a major tectono-magmatic event, the High Arctic Large Igneous Province (HALIP; Figure 1a). The term HALIP was initially presented by Tarduno (1998) and utilized by Maher (2001) for describing the Early Cretaceous magmatic activity in Svalbard. HALIP comprises large volumes of mafic rocks emplaced across the circum-Arctic in the Early Cretaceous. Magmatic rocks related to the HALIP occur as sills, dykes, lavas and pyroclastic material in Svalbard, Franz Josef Land, the New Siberian Islands, Sverdrup Basin of Arctic Canada, northern Greenland and the offshore Alpha-Mendeleev Ridge (Figure 1b; Bédard et al., 2021; Buchan & Ernst, 2018; Dibner, 1998; Dockman et al., 2018; Døssing et al., 2013; Jowitt et al., 2014; Lu et al., 2022; Maher, 2001; Senger, Tveranger, et al., 2014). Most of these Arctic regions are difficult to access, making scientific research on HALIP challenging. Nevertheless, Svalbard with its year-round civilian airport and a centrally located university center offers the most accessible well-exposed HALIP rocks emplaced in lithologically variable host rock formations (Figure 1c).

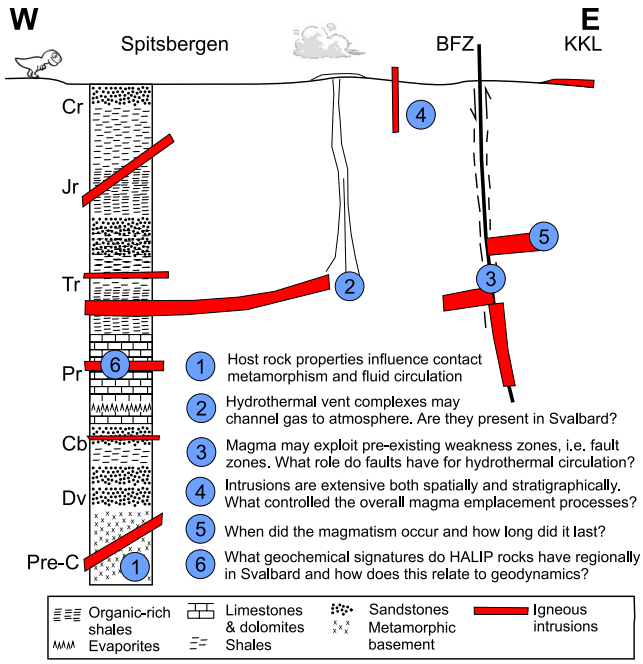

Figure 1. Schematic diagram illustrating important aspects of the motivation for studying High Arctic Large Igneous Province (HALIP) exposures in Svalbard. This study characterizes the extensive magmatism in central Spitsbergen, the most data-rich part of Svalbard. This is considered as a foundation to address these research questions in the entire Svalbard archipelago and other circum-Arctic HALIP sites. Numbers list scientific questions identified in this manuscript and indicate the locations in the HALIP plumbing system to address them.

There is an ongoing debate on whether HALIP can formally be classified as a LIP. The revised definition of LIPs by Bryan and Ernst (2008), also used by Bond et al. (2014), requires LIPs to be "aerially extensive (>100,000 km^2), volumetrically significant (>100,000 km^3 of magma), a maximum lifespan of ~50 Myr with intraplate tectonic settings or geochemical affinities and characterized by igneous pulse(s) of short duration (~1–5 Myr), during which a large proportion (>75%) of the total igneous volume has been emplaced." The apparent longevity of magmatism in Svalbard (Ar/Ar ages: ca. 75–145 Ma; U-Pb ages: 124.5 ± 0.4 Ma; Corfu et al., 2013; Senger, Tveranger, et al., 2014) and the pulsed HALIP-related magmatism in the Sverdrup Basin (at 122 ± 2 Ma, at 95 ± 4 Ma and at 81 ± 4 Ma; Dockman et al., 2018) suggest that HALIP may be too long-lasting to be a formally classified as a LIP. Further work complementing Shephard et al. (2016) linking the deep mantle structure, surface geology and process understanding of long-lasting mantle plumes capable of generating pulsed magmatism is required to decipher whether HALIP is truly a large igneous province or not. Regardless of this debate, in our study we use the broadest definition of HALIP following Maher (2001)—that is, as all high Arctic igneous rocks emplaced in the Early Cretaceous which, in Svalbard, are formally classified as the Diabasodden Suite (Dallmann et al., 1999).

In Svalbard, HALIP is manifested as predominantly basaltic sills and subordinary dykes of doleritic texture and Early Cretaceous age (Nejbert et al., 2011; Senger, Tveranger, et al., 2014). U-Pb dating from three localities in central-western Spitsbergen suggests a short magmatic pulse at 124.5 ± 0.4 Ma (i.e., early Aptian; Corfu et al., 2013). Lava flows are preserved only in eastern Svalbard on Kong Karls Land 300 km east of the study area (Bailey & Rasmussen, 1997; Olaussen et al., 2018). No lava flows are exposed in central Spitsbergen even though age-equivalent sedimentary strata (i.e., the Helvetiafjellet Formation) are well exposed, suggesting that there may be a regional control on the emplacement depth with magma only reaching the surface in far-eastern Svalbard and Franz Josef Land. Igneous intrusions of Early Cretaceous age are also interpreted on offshore seismic data south-east of Svalbard (Grogan et al., 2000; Polteau et al., 2016), where a 200,000 km^3 sill complex covering 900,000 km^2 has been mapped by Polteau et al. (2016).

While igneous intrusions are present over large parts of the Svalbard archipelago and the circum-Arctic, major knowledge and data gaps remain. One of the most critical data gaps relates to the timing and duration of HALIP magmatism. So far, only three reliable U-Pb dates are available from Svalbard, suggesting a short-lived magmatic pulse affecting Svalbard at ca. 124.5 Ma (Corfu et al., 2013). In contrast, K-Ar ages suggest an apparent long emplacement period between 198 and 98 Ma (Burov et al., 1977). Such prolonged magmatic activity is inconsistent with the LIP definition requiring a maximum duration of 50 Ma with most magmatism within a 5 Ma interval (Bryan & Ernst, 2008). Further afield, U-Pb geochronology in the Sverdrup Basin testify to multiple emplacement pulses (Dockman et al., 2018; Evenchick et al., 2015; Kingsbury et al., 2017). Timing and duration of magmatism is crucial when considering how rapidly greenhouse gases were liberated during contact metamorphism, and to what extent a given large igneous province may have influenced climate. Polteau et al. (2016) estimate that up to 20,000 Gt of carbon were generated during Early Cretaceous magmatism in the Barents Sea, but it is crucial to understand whether this amount was generated over a short or long period, and which proportion was released into the atmosphere.

The products of contact metamorphism induced by intrusive complexes feeding lavas of LIPs vary considerably depending on the lithology of the transformed rock. 3D seismic data offshore mid-Norway show that contact metamorphism in organic-rich shale can produce and release large volumes of methane and CO_2 through hydrothermal vent complexes (Svensen et al., 2004). Contact metamorphism of petroleum-bearing evaporites and organic rich shales in Siberia generated toxic components, such as methyl chloride and methyl bromide (Svensen et al., 2009). Note however that methane and CO_2 release to the atmosphere is not systematic, as numerous basins hosting igneous sills emplaced in organic-rich formations do not exhibit any hydrothermal vent complexes (de

Miranda et al., 2018; Spacapan et al., 2018, 2019). Assessing the nature of the environmental effects of large igneous provinces thus requires a solid knowledge of the lithology of the host rock of the LIPs plumbing system, the documentation of fluid release structures and good control on the composition and emplacement history of the magma.

In Svalbard, the documentation of contact metamorphic aureoles is presently missing from petroleum exploration boreholes, even though at least five of the boreholes penetrate igneous intrusions (Senger et al., 2019; Senger, Tveranger, et al., 2014). More importantly, these boreholes penetrate intrusions emplaced in diverse host rocks lithologies that vary from carbonates and evaporites to siliciclastic deposits including organic-rich mudstones and thus provide an excellent case study for addressing how host rock lithology influences contact metamorphism. However, no work has systematically and quantitatively addressed the stratigraphic range affected by the Diabasodden Suite magmatism.

Another knowledge gap relates to the mechanisms of magmatic emplacement, particularly when magma intruded a mechanically heterogeneous host rock like that present in Svalbard (Figure 1), both regionally and locally. Furthermore, the interaction of magma with pre-existing fault zones is poorly known. These larger-scale factors will, among others, control the spatial distribution of the magmatism (e.g., Schofield et al., 2015; Spacapan et al., 2016), which is critical to quantifying magma emplacement volumes.

In this contribution we integrate all available data to provide the first quantitative estimate of the spatial and stratigraphic extent of extensive HALIP-related magmatism in central Spitsbergen, the most data-rich part of Svalbard. In particular, we provide evidence of contact metamorphism in a range of lithologically varying host rocks using borehole data and discuss the potential for atmospheric de-gassing of the contact metamorphic aureoles. Furthermore, we place these new data within the context of remaining knowledge gaps, and advocate for the use of Svalbard as an accessible field laboratory for revealing HALIP magmatism.

2. Study Area and Geological Setting

Igneous intrusions of Early Cretaceous age (i.e., the Diabasodden Suite; Dallmann et al., 1999; Senger et al., 2014) are exposed in the high Arctic archipelago of Svalbard (Figures 2b and 2c). The study area covers ca 11,000 km^2 in the central part of Spitsbergen, the largest island of the archipelago. The region is well covered by onshore and offshore 2D seismic and exploration well data (Figures 2b and 2c). The onshore studies were carried along a 50 km wide and 130 km long, NW-SE oriented belt of vegetation-free, well-exposed and nearly continuous Upper Paleozoic-Mesozoic succession intruded by dolerite sills and dikes (Figure 2c). Offshore studies cover the major part of Isfjorden and smaller branching fjords (Figure 2). Major long-lived N-S oriented fault zones, notably the Billefjorden Fault Zone (BFZ) and the Lomfjorden Fault Zone (LFZ), transect the study area.

The geological evolution of Svalbard is well covered in the literature (Dallmann, 2015; Steel & Worsley, 1984; Worsley, 2008) and include several tectono-magmatic events affecting the host rocks (Figure 3). The basement in Svalbard consists of Proterozoic to Early Paleozoic metamorphic, igneous and unmetamorphosed sedimentary rocks that consolidated during the Caledonian orogeny (Dallmann, 2015; Gee & Tebenkov, 2004). Birkenmajer and Morawski (1960) report Early Cretaceous dolerite dykes within the Neoproterozoic to Cambro-Ordovician metamorphic and meta-sedimentary basement rocks in southern Spitsbergen, the stratigraphically deepest host rock. These particular dykes are distant from the only extrusive lava flows on Kong Karls Land (Olaussen et al., 2018), and likely represent feeder systems to the sill-dominated igneous complex intruding the Mesozoic strata in the central Spitsbergen study area.

Following the Caledonian orogeny, the Devonian Old Red Sandstone succession was deposited in major fault-bounded basins exposed in northern Svalbard (Braathen et al., 2018). The Ellesmerian (locally called Svalbardian) compressional event affected Svalbard during the Late Devonian (Piepjohn, 2000). The Late Carboniferous was dominated by localized rifting along major north-south trending tectonic lineaments, exemplified by the Billefjorden Trough filled with mixed siliciclastic-carbonate-evaporitic deposits, including the Ebbadalen Formation (Smyrak-Sikora et al., 2018, 2021). A tectonically stable platform was established by the Permian and lasted until the Late Jurassic. The transition from warm-water carbonates of the Gipshuken Formation (Blomeier et al., 2009) to cold-water carbonates of the Kapp Starostin Formation (Blomeier et al., 2013) during the Permian was facilitated by Svalbard's rapid northward drift. The Permian-Triassic boundary is well exposed in Svalbard (Zuchuat et al., 2020) and reveals a major mass extinction related to the Siberian Traps magmatism, driven also

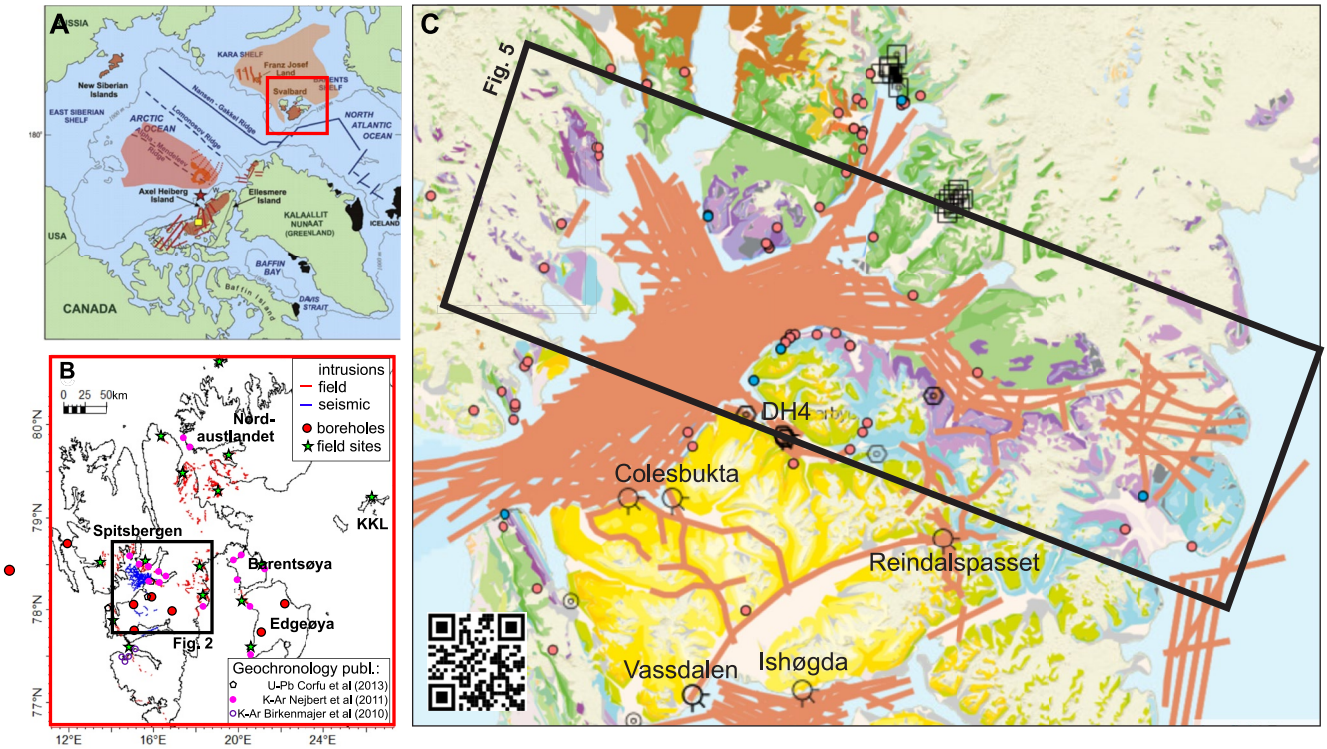

Figure 2. (a) Tectonic and geographic setting of Svalbard in the context of circum-Arctic High Arctic Large Igneous Province exposures and the main tectonic elements; figure modified from Kingsbury et al. (2017). (b) Overview map of the Svalbard archipelago illustrating the known intrusion extent and spatial extent of geochronological data (Birkenmajer et al., 2010; Corfu et al., 2013; Nejbert et al., 2011). FJL, Franz Josef Land; KKL, Kong Karls Land. (c) Geological map of the study area, highlighting the location of the exploration and research boreholes, 2D seismic coverage (orange lines) and virtual outcrop models of key field sites. Geological and topographic map courtesy of Norwegian Polar Institute made available through the open access Svalbox portal (Senger et al., 2020). The QR code can be used to directly access the digital interactive map available at www.svalbox.no/map.

by greenhouse gas liberation from the igneous complex feeding the Siberian Traps (Burgess et al., 2017; Li et al., 2021; Svensen et al., 2009).

The Triassic was dominated by siliciclastic deposition, beginning with Lower Triassic deltaic to offshore Vikinghøgda/Tvillingodden formations. The Middle Triassic organic-rich mudstones of the Botneheia Formation form a major host rock for the igneous intrusions investigated in this study (TOC up to 11%; Krajewski, 2013; Wesenlund et al., 2021). The overlying Tschermakfjellet and De Geerdalen formations comprise sandstones, siltstones and shales deposited in deltaic and fluvial environment (Olaussen et al., 2019). Sandstones and conglomerates of the Late Triassic-Middle Jurassic Wilhelmøya Subgroup form a major reservoir across the Barents Shelf and were also studied as the main target aquifer for a CO_2 storage project near Longyearbyen (Mulrooney et al., 2019; Senger et al., 2015). Natural fractures are pervasive in the reservoir (Ogata et al., 2012). Thin igneous sills are locally present in both drill cores and outcrops (Senger et al., 2013; Senger, Planke, et al., 2014). The Agardhfjellet Formation forms the main cap rock of the aforementioned CO_2 laboratory project, and comprises a shale-dominated succession with high TOC content (locally of up to 12%; Koevoets et al., 2018). An igneous dyke cuts the reservoir-cap rock interface at Botneheia (Senger et al., 2013), penetrating an unknown distance into the Agardhfjellet Formation. It is the most shallowly emplaced igneous body in central Spitsbergen.

The Early Cretaceous was marked by a shift in the sedimentary patterns, with a northerly source of the fluvial-dominated Helvetiafjellet Formation (Grundvåg et al., 2017) and a regional tilting of Svalbard toward the south. This is caused by a major uplift to the north during the Early Cretaceous, related to regional-scale thermal doming associated with HALIP magmatism (Ineson et al., 2021). Igneous intrusions of the Diabasodden Suite have been characterized in detail in the vicinity of Longyearbyen, where they compartmentalize a reservoir-caprock system envisioned for CO_2 storage (Senger et al., 2013; Senger, Planke, et al., 2014). Senger, Tveranger, et al. (2014) reviewed the research history of the Diabasodden Suite, and point to, among others, challenges with respect to precisely dating the igneous complex. The more remote Canadian Arctic has, in the

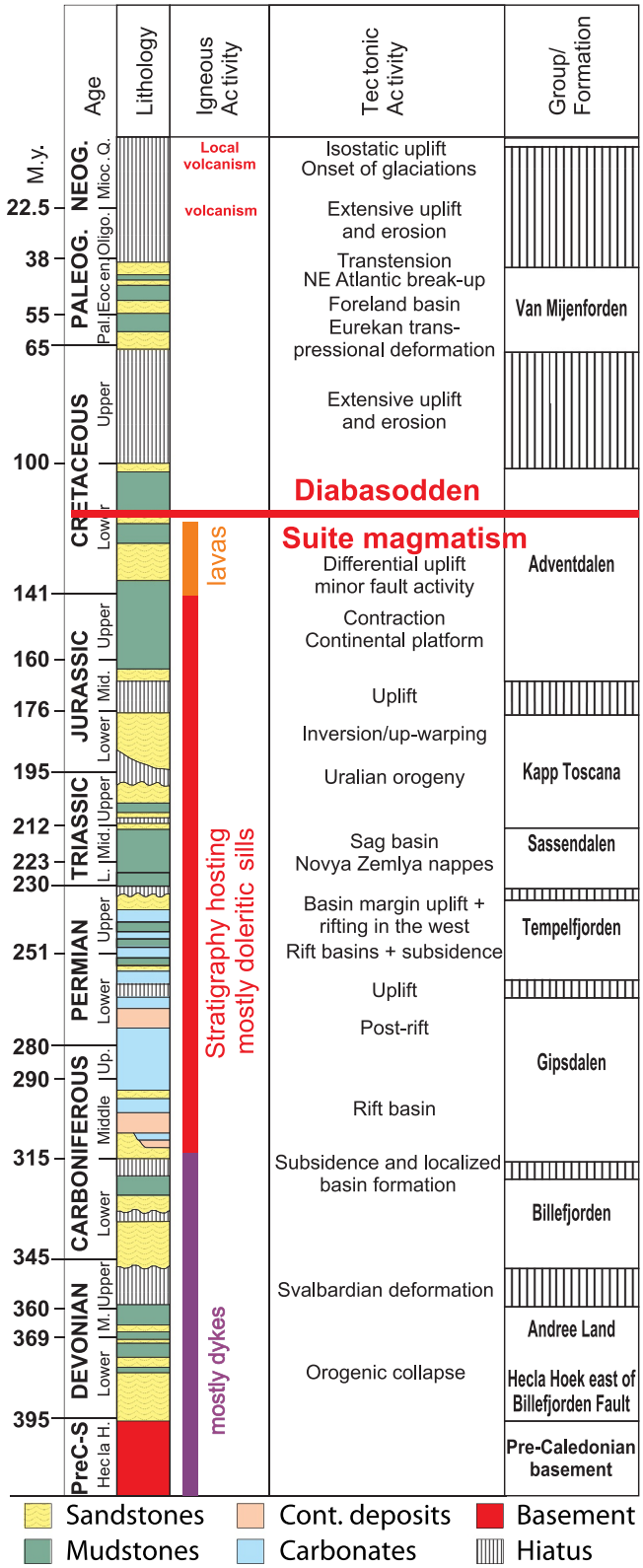

Figure 3. Regional stratigraphic column modified from Senger, Tveranger, et al. (2014) illustrating the major tectono-thermal events and the stratigraphy penetrated by the igneous intrusions of the Diabasodden Suite. Tectonic events updated after Olaussen et al. (2023).

same time, experienced major targeted research to characterize the HALIP intrusions in terms of geochronology (Dockman et al., 2018; Evenchick et al., 2015; Kingsbury et al., 2017), geochemistry (Kingsbury et al., 2016), ore mineralization potential (Saumur et al., 2016; Wilton et al., 2019) and tectono-stratigraphy (Schröder-Adams et al., 2019).

A major hiatus occurs in the Upper Cretaceous. Only reworked pollen of Middle to Late Cretaceous age indicate that Upper Cretaceous strata were present in Svalbard in the past (Smelror & Larssen, 2016). Paleogene coastal plain to deep water basin siliciclastic deposits overlie the hiatus (Helland-Hansen & Grundvåg, 2020). These sediments notably provide the backbone of Svalbard's infrastructure through the commercially exploited coal-bearing strata in the Firkanten Formation, which is still actively mined in Barentsburg and Longyearbyen (Senger et al., 2019). The Paleogene strata were deposited in the Central Spitsbergen Basin, a sedimentary basin formed in the foreland of the Paleogene West Spitsbergen Fold-and-Thrust Belt (WSFTB) located in the west (Bergh et al., 1997). The entire igneous complex of the Diabasodden Suite was affected by this major tectonic event, as evidenced by faulted and folded igneous intrusions at, for instance, Festningen and Mediumfjellet.

Another hiatus in sedimentary record of Svalbard occurs in the Neogene (Figure 2), with major glaciations and a pre-glacial tectonic and post-glacial isostatic uplift (Lasabuda et al., 2021). Magmatic activity, however, occurred in north-west Spitsbergen. It is manifested by both Miocene lava flows of the Seidfjellet Formation (Prestvik, 1978) and three volcanic centers of Quaternary age (the Bockfjorden Volcanic Complex; BCV) along the Breibogen Fault (Treiman, 2012). Both the propagation of spreading ridges some tens of kilometers offshore western Svalbard and proposed Miocene magmatism in the Sophia Basin north of Svalbard (Geissler et al., 2019) are likely to have had a pronounced effect on both uplift and thermal regime in western Svalbard since the Oligocene (Minakov, 2018). The BCV lavas contain 15%–20% mantle xenoliths (Grégoire et al., 2010), and provide evidence for conduits to the mantle under West Spitsbergen as late as the Quaternary along the N-S trending fault zone (Skjelkvåle et al., 1989).

The recent uplift affected the entire study area, with implications on reservoir quality and subsurface pressure systems. Olaussen et al. (2019), for instance, use vitrinite reflectance data to suggest that at least 2 km of overburden are missing near Longyearbyen. This general over-compaction of the sediments in the study area has practical implications for seismic mapping of igneous intrusions, as the acoustic impedance contrast between igneous intrusions and well-cemented host rocks is not as clear as in normally compacted basins (Rabbel et al., 2018).

3. Data and Methods

We integrate all available data (Table 1) to quantify the spatial and stratigraphic extent of the dolerites in the central Spitsbergen study area (Figure 2c).

3.1. Field and Geospatial Data

Field data relies on numerous field mapping campaigns conducted in the study area between 2011 and 2021, and in particular utilizes digital outcrop models (DOMs) for quantitative outcrop analyses of often inaccessible outcrops. DOMs are processed from georeferenced images ideally acquired

Geochemistry, Geophysics, Geosystems

10.1029/2021GC010300

Table 1
Summary of Data Sets Utilized in This Study

Data type	Onshore versus offshore		Coverage	Resolution and details	Application					Data source
	Onshore	Offshore			Spatial extent	Stratigraphic extent	Intrusion shape	Geochemistry	Aureole characterization	
Regional data sets										
Digital elevation model	X		Entire study area	20 m	X	X	X			Norwegian Polar Institute (2014a)
Geological maps	X		Entire study area	1:100,000	X	X				Norwegian Polar Institute (2014b) and Dallmann (2015)
Satellite imagery	X		Entire study area	c. 1 m	X		X			Norwegian Polar Institute (2014b)
2D seismic	X	X	Isfjorden, Van Mijenfjorden, partly onshore in main valleys	tens of m	X	X	X			Svalex, Equinor (Statoil and Norsk Hydro data), (Blinova et al., 2013; Bælum et al., 2012)
Aerial magnetic data	X	X	Entire study area	SPA-88 survey, 1,550 m sensor elevation, 4 km line spacing	X					NGU, (Dallmann, 2015; Skilbrei, 1992)
Gravity data	X	X	Entire study area							NGU, (Dallmann, 2015)
Local data sets										
Exploration boreholes	X		Five boreholes in study area, some with wireline logs	dm-scale for wireline data, no physical core available		X		X	X	NPD, NPN Senger et al. (2019)
Research boreholes	X		DH4, Adventdalen	cm-scale on core material		X			X	UNIS CO_2 lab project (Braathen et al., 2012; Olaussen et al., 2019; Senger, Planke, et al., 2014; Senger, Tveranger, et al., 2014)
Ship-based magnetic data		X	Isfjorden	50 m point spacing, line spacing c. 500 m	X					Svalex, Senger et al. (2013)
Digital outcrop models (DOMs)	X		All studied sites	Intrusion thickness and extent	X	X	X		X	Svalbox (Senger et al., 2020)
Field studies	X		Various field campaigns throughout study area	Intrusion geometry and architecture	X	X	X	X	X	Senger et al. (2013) and Sartell (2021)

Table 1
Continued

Data type	Onshore versus offshore: Onshore	Onshore versus offshore: Offshore	Coverage	Resolution and details	Application: Spatial extent	Application: Stratigraphic extent	Application: Intrusion shape	Application: Geochemistry	Application: Aureole characterization	Data source
Laboratory data sets										
Geochemical data	X		Boreholes, coastal locations	Major and minor elements Rock-Eval				X	X	Bro (2007a, 2007b, 2007c), Shkola (2007), and Nejbert et al. (2011)
Geochronological data	X		Central-western Spitsbergen, coastal locations	U/Pb geochronology on 3 samples,						Corfu et al. (2013), Firshov and Livshits (1967), and Gayer et al. (1966)

Note. NPD, Norwegian Petroleum Directorate; NPN, Norsk Polar Navigasjon; NGU, Geological Survey of Norway.

from a drone, processed using structure-from-motion (SfM) algorithms (e.g., Westoby et al., 2012) implemented in Agisoft's Metashape software and shared openly on the Svalbox geodata portal (Senger et al., 2021).

Digital terrain models and geological maps (Norwegian Polar Institute, 2014a) are integrated for a quantitative characterization of the intrusions exposed within the study area. The same data are used to generate a surface of the base of the Helvetiafjellet Formation, a proxy for the near-horizontal paleo-surface at the time of HALIP, in order to reconstruct the paleodepth of the intrusions at the time of their emplacement. The geospatial data are also used to classify the individual intrusions based on the intrusion geometry (exposure length, area coverage, elevation) and its relationship to the stratigraphy (host rock formation, age and lithology).

3.2. Borehole Data

Subsurface characterization relies on wireline data and reports from five onshore petroleum exploration boreholes in the area, which are tied to a regional 2D seismic database. The boreholes were drilled from 1965 to 1994 (Senger et al., 2019). None resulted in commercial hydrocarbon discoveries. Data sets from these vintage boreholes are fragmented but UNIS has in recent years compiled all available data (e.g., wireline logs, final well reports, cuttings, cores; Table 1) from the boreholes in a single Petrel project as part of the Svalbard Rock Vault and Svalbox projects. In addition to the petroleum exploration boreholes, a fully cored research well in Adventdalen, DH4, penetrated a 2.28 m thick igneous intrusion (summarized by Senger, Planke, et al. [2014]).

3.3. Seismic Data

The study area is covered by the densest 2D seismic grid in Svalbard, and likely anywhere this far north. This reflects both past petroleum exploration activity (in particular in the 1970s) and research efforts, including the annual Svalex expeditions (Saether et al., 2004), the Longyearbyen CO_2 lab project (Bælum et al., 2012; Olaussen et al., 2019) or the stratigraphic drilling at Sysselmannbreen (Johansen et al., 2011). Onshore acquisition was facilitated by the development of the snowstreamer (Eiken et al., 1989), but acquisition is nonetheless costly and restricted to the main valleys and easily accessible glaciers. The offshore grid is denser than onshore and covers the majority of Isfjorden and some of its tributaries. In this study, we integrate all available seismic data (Figure 2) and focus on mapping out high-impedance, locally discontinuous and cross-cutting reflectors that are classical signs of igneous intrusions (Planke et al., 2005) and that we attribute to the Diabasodden Suite. Marine seismic data, though hampered by the presence of a strong seafloor multiple, provide reasonable quality used to map igneous intrusions, major faults and thrust faults (Blinova et al., 2013; Roy et al., 2019; Senger et al., 2013). Quality of onshore data are hampered by the presence of permafrost but provide important well calibration and regional correlations (Anell et al., 2014).

3.4. Well-Seismic Correlation

The boreholes provide an important calibration point for seismic interpretation. Only one of the petroleum boreholes, Reindalspasset, was drilled based on 2D seismic data acquisition (Senger et al., 2019). In addition, 2D seismic data acquired after drilling are available over the Vassdalen and Colesdalen boreholes and in the near vicinity of the Ishøgda borehole (Figure 1). We use a simple velocity model (constant 4 km/s reflecting the overcompacted sediments; Bælum & Braathen, 2012) to tie the boreholes to the seismic data. Some depth uncertainty is thus expected when visualizing well data on time sections along with seismic data.

3.5. Magnetic Data

The 2D seismic interpretation is integrated with regional-scale aeromagnetic data (Dallmann, 2015) and a ship-based magnetic survey in Isfjorden (Senger et al., 2013). The

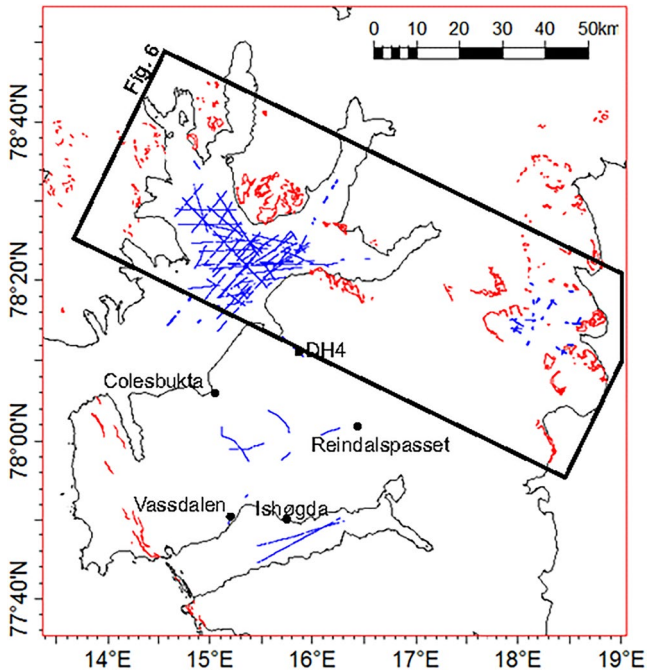

Figure 4. Regional distribution of igneous intrusions in the study area, mapped onshore (red) and interpreted on seismic (blue).

ship-based magnetic data was processed by Gernigon (NGU) and is described in Senger et al. (2013). The magnetic data confirm the presence of magnetic intrusions and expand the spatial coverage of the 2D seismic data.

3.6. Gravity Data

Regional gravity data (Dallmann, 2015) provides the structural framework for this study, by identifying the major basins and highs in central Spitsbergen, such as the Central Spitsbergen Basin. No targeted gravity surveys were conducted to map out the igneous intrusions in the study area.

3.7. Igneous Geochemistry

Previously unpublished whole rock geochemical data of dolerite samples are also reported for two Russian exploration boreholes at Vassdalen (Bro, 2007c) and Colesbukta (Shkola, 1977, 2007). These are integrated with published geochemical data from outcrops to link the borehole intrusions with the outcrops.

4. Results

We first present the spatial extent of the igneous intrusions in the study area, integrating primarily field and seismic data (Figure 4). Then we discuss the stratigraphic distribution of the intrusions as seen in field, seismic and in particular borehole data. Finally, we link outcrops and borehole intrusions through previously unpublished geochemical data.

4.1. Intrusion Shapes and Spatial Extent: Integration of Field Mapping and Seismic Data

The igneous intrusions are widespread throughout Svalbard (Figure 5) and occur across virtually the entire study area from Oscar II Land to the East Coast (refer to Figure 4 for placenames). Most intrusions observed in the field and on seismic data are flat-lying sill complexes, which consist dominantly of segments that are concordant with the sedimentary strata of the host rock, with local discordant segments. Dykes are present locally, typically 2–10 m in thickness, and are observed in the field and on offshore magnetic data. Due to the low thickness and sub-vertical orientation we do not expect dykes to be imaged by 2D seismic data. Seismic interpretation and

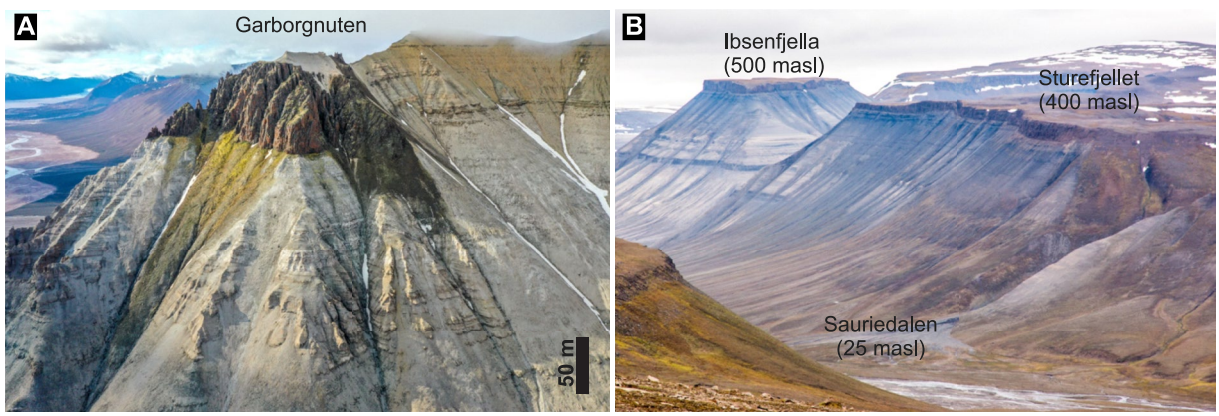

Figure 5. (a) Drone photograph of a spectacularly exposed dolerite sill at Garborgnuten mountain, Dickson Land. The sill formed near the boundary between the gypsum-bearing Gipshuken Formation (layered white strata below) and the Kapp Starostin Formation (yellow strata). Note that the sill does not extend to the right of the image but climbs along a subvertical step (photo courtesy: Rafael Horota). (b) Field photograph of a ca. 40 m thick dolerite sill (brown cliff and layer topping the mountain) observed at Sauriedalen, viewed toward the north-east. The host rock consists of the organic-rich shale of the Botneheia Formation. Individual sills in the area are exposed for over 10 km.

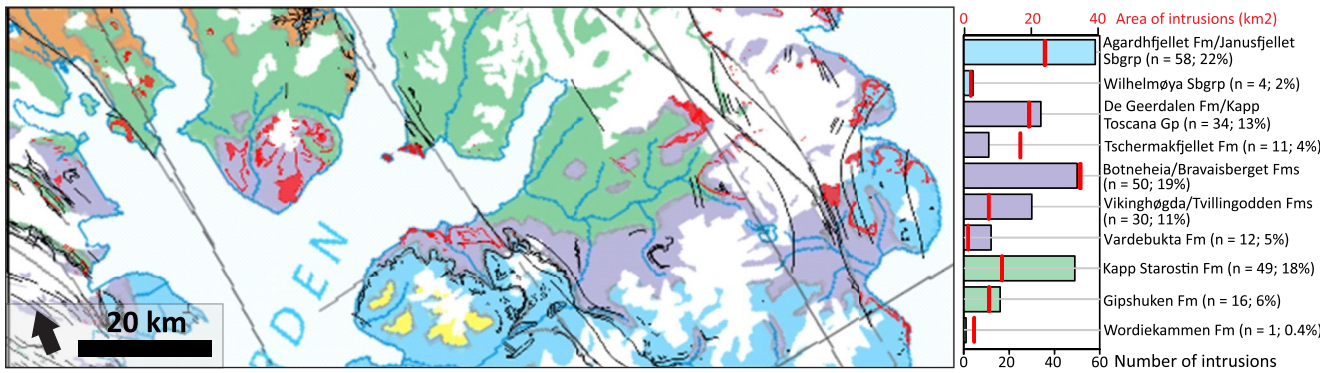

Figure 6. Distribution of dolerite intrusions within the study area (red), as mapped at 1:100,000 scale by the Norwegian Polar Institute (Dallmann, 2015). The bar chart to the right reveals the host rock distribution for all 265 intrusions exposed in the study area. The red bars indicate the total cumulative area of intrusions within each formation.

borehole data confirm igneous intrusions in Mesozoic strata beneath the Paleogene succession. Within the ca 11,000 km^2 large study area, igneous intrusions directly cover 72 km^2 and are inferred from a 3,200 km^2 large subsurface area (i.e., 29% of the study area).

4.1.1. Field Exposure: Spatial Extent and Stratigraphic Distribution

The 130 by 50 km (i.e., 6,500 km^2) large field area illustrated in Figure 6 is dominated by Permian-Cretaceous host rocks. We aim to quantify where the igneous intrusions were emplaced and, specifically, if there is a preferential emplacement in mechanically weak strata such as the Late Jurassic and Middle Triassic organic-rich shales. Approximately 29% of the study area (1,915 km^2) is covered by fjords. Of the remaining land area (4,575 km^2), exposed igneous intrusions of the Diabasodden Suite cover 1.6% (72 km^2). It must be noted that numerous igneous intrusions are not mapped at the 1:100,000 scale as identified during field work, so this represents a minimum area of igneous intrusions.

The stratigraphic distribution of the 265 mapped Diabasodden Suite intrusions within the study area is illustrated in Figure 6. The majority of intrusions are emplaced within the shale-dominated Agardhfjellet (22% of all intrusions) and Botneheia (19%) formations, as well as the spiculitic Kapp Starostin Formation (18%). Other significant host rocks are the heterolithic siliciclastic De Geerdalen (13%) and Vikinghøgda/Tvillingodden (11%) formations. The thin sandstone-dominated Wilhelmøya Subgroup only hosts 2% of the intrusions, while the carbonate-dominated Gipshuken Formation hosts 6% of intrusions. Considering the cumulative area of the igneous intrusions rather than the amount of intrusions the Botneheia Formation is the dominant host rock with ca 35 km^2 of intrusions. Notably, the Kapp Starostin Formation only hosts 11 km^2 of intrusions, even though in terms of a number of intrusions it is comparable with the Botneheia Formation. As such, we confirm that the largest intrusions are preferentially emplaced in the organic-rich shales of the Agardhfjellet and Botneheia formations.

An important unknown is the main feeding structures of the igneous intrusions as dykes are only rarely observed in the field. A hypothesis is that the major fault zones in the study area have been used to channel magma transport across the crust. To test this hypothesis, we correlate the area of the exposed intrusions with distance to major faults (i.e., those mapped at 1:100,000 scale; Figure 7). Grouping all intrusions together irrespective of the host rock stratigraphy, there is a clear increase in number of igneous intrusions within 2 km of the nearest fault zone. The number of intrusions is relatively stable between 2 and 10 km from faults, and no igneous intrusions are located >14 km from fault zones. Clearly there is some bias within the relatively small study area but the data nonetheless suggest that there may be a relationship between igneous intrusions and fault zones.

The individual intrusions' area spreads over several orders of magnitude (Figure 7). The intrusion areas are plotted as box whisker plots subdivided by the host rock formation to illustrate the area range and mean area for each host rock (Figure 6a). The means, with the exception of the undersampled Wordiekammen Formation with only one intrusion, fall within a 0.01–1 km^2 range. From the three major host rocks, the Botneheia Formation offers somewhat larger individual intrusions than in the Agardhfjellet and Kapp Starostin formations, but also a broader range from minimum to maximum. Clearly, the exposed intrusion areas only represent the minimal extent

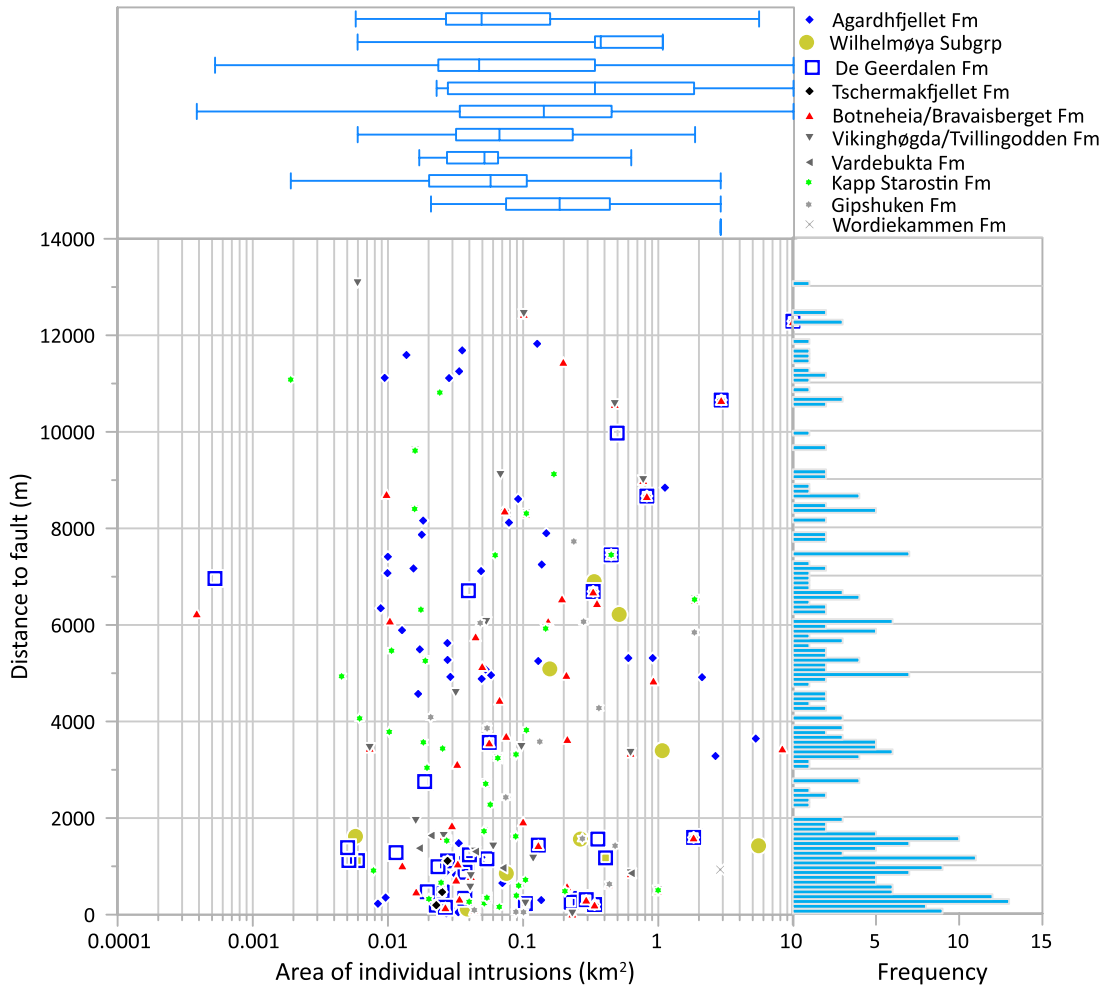

Figure 7. Cross-plot investigating relationships between intrusion size and distance from faults for 265 mapped intrusions emplaced in different host rocks. The histogram illustrates the distance to mapped fault systems from the igneous intrusions, with 100 m wide bins. The Box-whisker plots illustrate the range of exposed area (minimum, lower quartile, mean, upper quartile and maximum) for the 265 intrusions emplaced in the different host rocks.

of magmatism in the study area, with the majority of sills covered in the terrain. Nonetheless, the distribution of intrusion areas within the different formations may reflect regional-scale mechanical properties of the host rocks.

4.1.2. Subsurface Characterization of Igneous Intrusions

We have interpreted all available 2D seismic lines, using the exploration boreholes to guide the seismic interpretation to constrain the spatial extent of the igneous intrusions (Figure 8). We focus primarily on identifying high-amplitude, locally discontinuous and cross-cutting reflectors. It must be noted that the high velocities of the host rocks reduce the acoustic impedance contrast with high-velocity igneous intrusions compared to normally compacted basins. In addition, many of the drilled intrusions are relatively thin (<10 m) and thus considered to be below seismic resolution.

Igneous intrusions confirmed in Middle Triassic strata by the Colesbukta and Vassdalen wells can be interpreted some distance away from the wells (Figure 9). Figure 9 ties the two wells in a 40 km long N-S section underlying the Paleogene succession. The profile suggests that the intrusive complexes could be spatially linked, though the sub-optimal seismic quality and thin intrusions pose some uncertainty. Field studies suggest that individual igneous intrusions may extend for up to 30 km long (Senger, Tveranger, et al., 2014).

Igneous intrusions are also interpreted eastwards from Vassdalen toward the Ishøgda borehole on an offshore seismic line in Van Mijenfjorden (Figures 8–10). Here the intrusive complex appears at least 20 km long, conformable with the regional dip of the Paleogene succession. At the eastern end of the interpreted sill, acoustic blanking

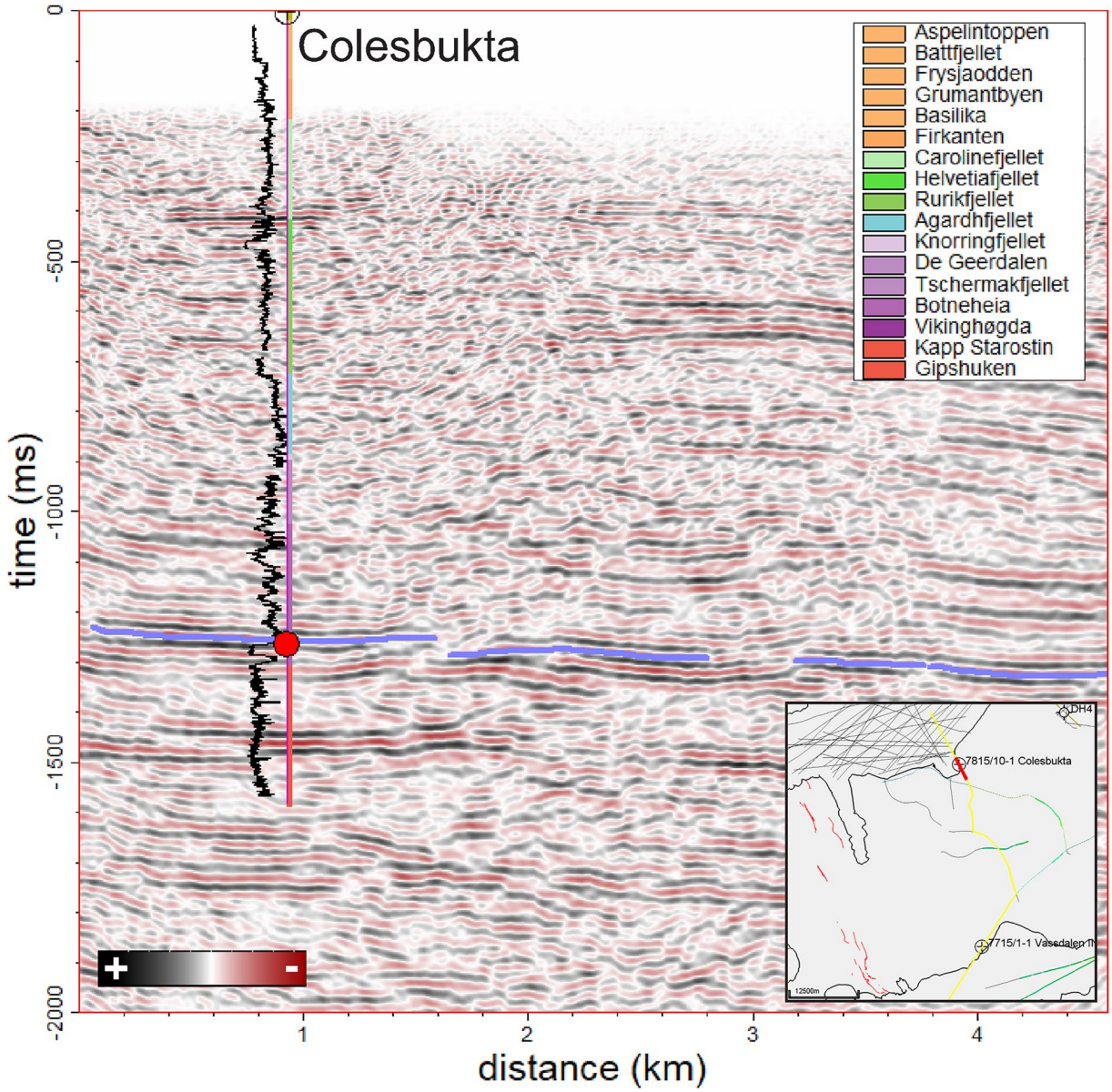

Figure 8. First-order well-seismic correlation across the Colesbukta petroleum exploration borehole, utilizing a constant velocity model (4 km/s) reflecting the overcompacted high-velocity sediments (Bælum & Braathen, 2012). The red circles highlight the location of the sill in the borehole. The discrete log represents the penetrated strata, and the gamma ray log is also shown to facilitate lithological identification.

above the sill's termination could indicate de-gassing through pipes or hydrothermal vent complexes. However, high-resolution 3D seismic data would be required to confirm this.

Offshore 2D seismic data in Isfjorden provide very good coverage and better quality than onshore seismic data. Figure 10 illustrates an example of a SW-NE section with widespread igneous intrusions. The dense 2D grid in Isfjorden allows detailed mapping of the intrusive complex and a reliable interpretation of its extent as shown in Figure 4.

4.1.3. Magnetic Map

The seismic interpretation is complemented by aerial magnetic data (Figure 12). The magnetic data are relatively regional but provided an additional spatial extension to the 2D seismic interpretation. In particular, the circular magnetic high in the inner part of Isfjorden is likely attributed to be at least partly caused by the igneous

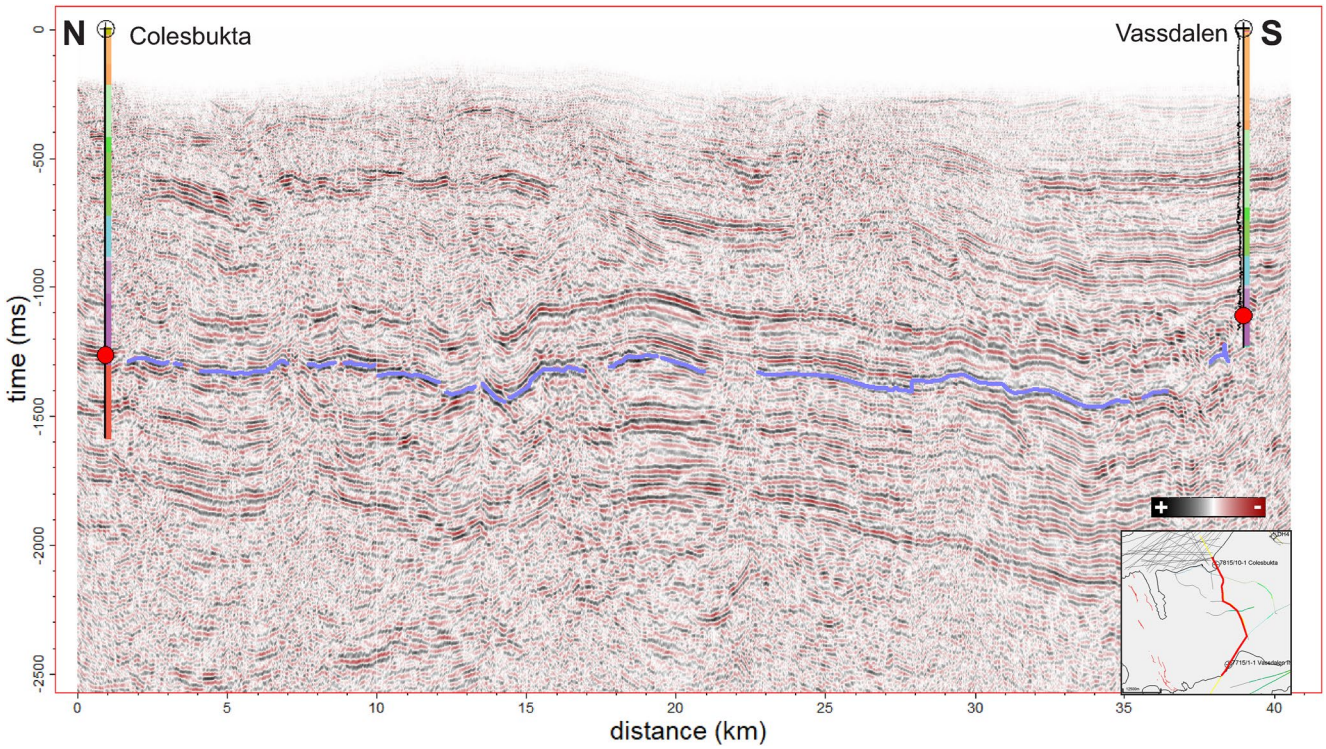

Figure 9. Composite onshore seismic line (NH9108-04; NH9108-05; NH9108-07) linking the Colesbukta and Vassdalen boreholes, highlighting the igneous intrusions encountered in the boreholes (red circles) and interpreted on the 2D seismic (blue line). Legend for formations on well logs is provided in Figure 8.

intrusions. The magnetic high spatially overlaps with the major igneous centers at Diabasodden and southern Dickson Land and the seismic interpretation of the igneous complex.

Furthermore, ship-based magnetic data in inner Isfjorden as presented by Senger et al. (2013) indicate direct correlation of magnetically high anomalies offshore with igneous dykes onshore. The ship-based magnetic data confirms the extent of the central Spitsbergen igneous complex across Isfjorden (Figure 12d). A strong magnetic anomaly links the Hatten-Diabasodden area to the Rotundafjellet area on the northern shore of Isfjorden. Indeed, there is a ca 10 m thick dyke exposed at the beach beneath Rotundafjellet that may be related to the magnetic anomaly (Figure 12e).

In addition, more scattered magnetic anomalies occur along the regional ca, 3 km wide WNW-ESE trending belt along which igneous intrusions are exposed from the Billefjorden Fault Zone to Hatten. It is likely that many of these magnetic anomalies are also caused by the presence of igneous intrusions.

4.2. Stratigraphic Distribution and Emplacement Depth/Thickness of the Intrusions

The lithologies, and so the stratigraphy, affected by igneous activity, and the depth at which the intrusions were emplaced, must be constrained in order to assess the effects of contact metamorphism, which affects different host rock lithologies to a varying extent. We utilize primarily borehole date to quantify the emplacement depth and affected stratigraphy, and use field and seismic data to complement the borehole data in a regional setting.

Boreholes, particularly if fully cored (DH4; Senger, Planke, et al., 2014) or with adequate wireline logs (Ishøgda, Reindalspasset), are obvious targets to characterize intrusion and aureole characteristics. In addition, by assuming the base of the Helvetiafjellet Formation as an approximation for the paleo-topography, the paleo-emplacement depth can be estimated (Table 2).

Igneous intrusions are confirmed in five onshore exploration boreholes and one research borehole within the study area (Figure 13). The majority of the intrusions occur in Triassic shale-dominated strata, in particular in the Middle Triassic Botneheia Formation. The stratigraphically deepest borehole, Reindalspasset, also penetrates

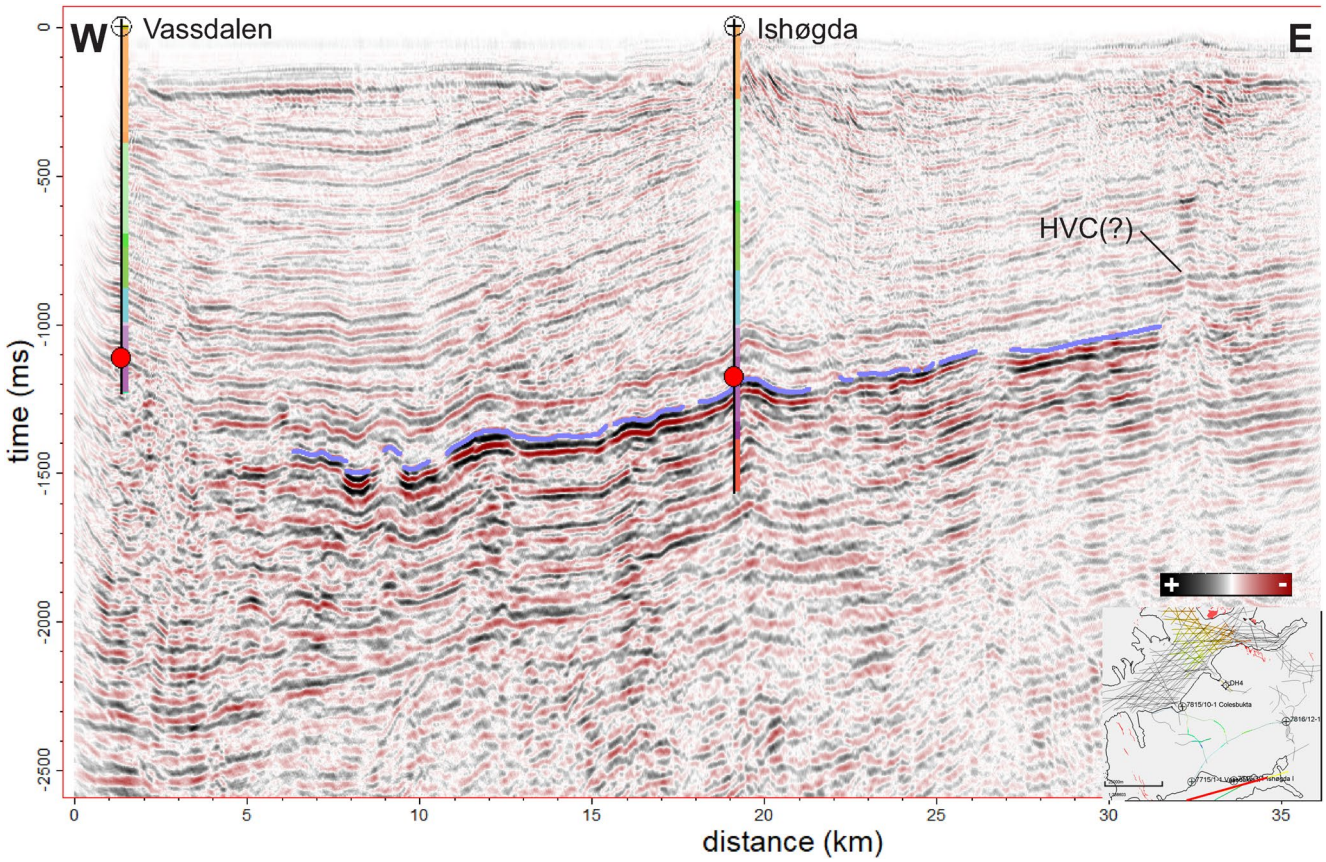

Figure 10. Offshore seismic line NH8510-203 in Van Mijenfjorden, providing a regional and Vassdalen boreholes, highlighting the igneous intrusions encountered in the boreholes (red circles) and interpreted on the 2D seismic (blue line). The feature to the east of the sill could potentially represent a de-gassing structure such as a hydrothermal vent complex (HVC), but higher-quality 3D seismic data is required to resolve this. Legend for formations on well logs is provided in Figure 8.

an intrusion in the sandstone-dominated Ebbadalen Formation (Figure 13). Intrusions in boreholes range from 2 to 61 m in thickness, with an average thickness of 16 m (Table 2). The intrusions are emplaced 715–1,850 m beneath the paleo-surface.

4.3. Aureole Characterization

Detailed characterization of contact metamorphic aureoles is critical in the context of potential environmental change associated with igneous activity. This is especially important when an igneous event affects lithologically highly variable host rocks, as it occurred in Svalbard. Ideally, intrusions and both upper and lower aureoles are fully cored and Rock-Eval characterization can be conducted to quantify how much of the host rock is affected with respect to intrusion thickness. In the study area, this is only possible in the DH4 research borehole in Adventdalen which was characterized by Senger, Planke, et al. (2014). The following sections describe previously unavailable wireline data to characterize aureoles in both Carboniferous sandstone and Triassic shale-dominated strata.

4.3.1. Intrusion in Siliciclastic Carboniferous Strata: 7816/12-1 Reindalspasset

A 21 m thick intrusion was penetrated by the 7816/12-1 petroleum exploration borehole drilled by Norsk Hydro (now Equinor) at Reindalspasset in 1991. The intrusion is emplaced in the Ebbadalen Formation, a heterolithic succession comprising siliciclastics, evaporites and carbonates that is only present within mid-Carboniferous half-grabens such as the Billefjorden Trough exposed ca. 70 km north of the borehole. Interestingly, no igneous intrusions were reported in recent field-based studies from the Billefjorden Trough (Smyrak-Sikora et al., 2018, 2021), though some igneous rocks of unknown age were reported from mine ventilation shafts in the vicinity of Pyramiden (Verba, 2015).

In the borehole, the intrusion is clearly distinguished from the host rock on the basis of the low Gamma Ray (GR) and high velocity and density values (Figure 14). Aureoles are defined primarily using sonic data, with the lower aureole in particular showing a gradual increase in P-wave velocity from the background trend (ca. 4.7–5.5 km/s) to the intrusion (5.6–6.6 km/s).

Rock-Eval data indicate that the total organic content (TOC) in the host rock is minimal within 50 m near the intrusion (<0.1%), and only increases in the shaly and coaly Billefjorden Group beneath from ca. 2,260 m depth (Figure 14). The very low TOC of the host rocks is likely a combination of initially minimal organic matter in the paralic sediments, deep burial and perhaps some intrusion-related maturation. However, the data clearly cannot be used to characterize an aureole based on geochemical data.

4.3.2. Intrusions in Middle Triassic Strata

Igneous intrusions are preferentially emplaced in mechanically weak shale-dominated succession, which in central Spitsbergen is often provided by the Triassic Botneheia, Tschermakfjellet and De Geerdalen formations. The DH4 research borehole in Adventdalen fully cored a 2.28 m thick igneous intrusion, and a contact aureole of 160%–195% of the intrusion thickness was characterized on the basis of Rock-Eval pyrolysis (Senger, Planke, et al., 2014).

Figure 15 highlights the igneous intrusions in three petroleum exploration boreholes with a different suite of wireline logs. All are emplaced in Triassic organic-rich mudstones where significant gas generation is expected. The relatively thin sills in the two adjacent Vassdalen boreholes are not clearly discernible in the wireline data, through the intrusion itself offers a high resistivity. The Ishøgda borehole exhibits a thin and a thick sill. The thick sill is clearly discernible on the wireline data, with low gamma ray and high resistivity and velocity. Notably, both contact aureoles are characterized by very low resistivity, which may be related to inter-connected pyrite or graphite as described recently from the Neuquén Basin by Spacapan et al. (2019). A similar signature, though only in the lower aureole, is apparent in the Colesbukta borehole (Figure 15).

4.4. Geochemical Signature of Drilled Intrusions

The geochemical signature of the DH4 and Colesbukta boreholes overlap with previously published geochemical analyses of the Diabasodden Suite outcrops (Nejbert et al., 2011; Shipilov & Karyakin, 2011), as illustrated by the TAS diagram of Figure 16. The Vassdalen stacked intrusions show a larger SiO_2 variation, but also here the majority of samples suggests a basaltic affinity. Most likely, all these drilled intrusions are related to the Early Cretaceous magmatism and can be classified as part of the Diabasodden Suite. No geochemical data is available from the Reindalspasset borehole as the sidewall core targeting the intrusion misfired.

5. Discussion

5.1. Magma Volumes in Central Spitsbergen: Comparison With HALIP

It is crucial to understand how much magma was emplaced, when, and into what kind of host rock lithologies to discuss potential climate perturbations of the igneous activity.

We quantified magma volumes in arguably the most data-rich part of the HALIP, where adequate seismic, borehole and excellent field exposures are abundant. The presented estimates are thus considered to be more precise than the regional coarse estimates presented from other HALIP provinces (Table 3). We confidently characterize 72 km^2 of igneous intrusions in the field area, which represents 0.14–2.5 km^3 of magma volume depending on the aggregate sill thickness used (2–35 m). The subsurface extent of the intrusions is unsurprisingly an order of magnitude higher, with borehole and seismic data confirming intrusions across an area of 3,200 km^2. On a regional scale, Diabasodden Suite exposures are known from Sørkapp to Nordaustlandet, and from western Spitsbergen to Kong Karls Land (Birkenmajer et al., 2010; Nejbert et al., 2011; Senger, Tveranger, et al., 2014). A rough estimate indicates that at least 120,000 km^2 is affected by magmatism in Svalbard and its near vicinity (Table 3). Depending on the assumptions on regional aggregate sill thickness, 1,200–10,000 km^3 of magma are present in the Svalbard area (Maher, 2001; this study). Grogan et al. (2000) and Polteau et al. (2016) expand the focus regionally toward the south-east, where seismic data indicate igneous sills over significant parts of the

Barents Shelf, totaling up to 900,000 km^2 (200,000 km^3 in volume) if the onshore exposures of Svalbard and Franz Josef Land are included.

In comparison, the Sverdrup Basin is affected by aerially somewhat less extensive magmatism, but the overall much thicker sills suggest a larger overall magma volume exceeding 100,000 km^3 (Saumur et al., 2016; Table 3) than occurring onshore and near-shore Svalbard (1,200–10,000 km^3). No detailed spatial and volume assessments are available for the other HALIP provinces, including northern Greenland and the New Siberian Islands. The offshore Alpha-Mendeleev magnetic high that is partly attributed to igneous activity, however, extends over several orders of magnitude more than all the onshore HALIP provinces together. There is no threshold volume in terms of magmatic emplacement over time (i.e., magma emplacement rates) that would lead to profound effects on global climate as many factors contribute here, including host rock properties (e.g., maturation stage, organic richness, presence of petroleum, porosity), magma emplacement (e.g., temperature, rates, geometry, emplacement depth etc.) and atmospheric release of generated greenhouse gasses (e.g., hydrothermal venting, marine/terrestrial release, atmospheric circulation during emplacement). However, geologically rapid and catastrophic intrusion of large magma volumes as documented for the Siberian Traps (Burgess et al., 2017; Svensen et al., 2009) would certainly have a larger impact than long-lived intrusion of low magma volumes.

The timing of the magmatism is thus crucial to constrain magma emplacement rates and scrutinize potential atmospheric effects. In this respect, the lack of reliable, regional and numerous geochronological constraints is problematic, and discussed as a major knowledge gap below. The U/Pb method provides reliable age constraints, as illustrated by regional geochronological constraints of the Karoo LIP emplaced at 183.0 ± 0.5 to 182.3 ± 0.6 Ma (Svensen et al., 2012). The 14 samples in the Karoo LIP were collected from sills and dykes over a distance of up to 1,100 km, with a remarkable short time span of emplacement of about 0.47 Myrs (Svensen et al., 2012). Such rapid emplacement will undoubtedly result in stronger climatic perturbations than prolonged more diffuse magmatism.

In Svalbard, only three samples provide reliable U/Pb ages, centered at 124.5 Ma (Corfu et al., 2013). Ongoing U/Pb dating of dolerites from Ekmanfjorden is in agreement with this older pulse (Anna Sartell, pers. comm. October 2022; Sartell, 2021). In contrast, U/Pb dating of six samples in the Sverdrup Basin by Dockman et al. (2018) was integrated with previously published samples to indicate a pulsed event, with three main magma emplacement pulses (124–120, 99–91, 85–77 Ma; Table 3). Whether the two later pulses are present in Svalbard or not is unknown. Clearly, more targeted geochronological work is required to constrain the timing of magmatism, its duration and consequently magma emplacement rates.

5.2. Emplacement Depth, Contact Metamorphism, and Potential for Atmospheric Degassing

The large volumes of lava erupted during a LIP can release immense volumes of CO_2 (Courtillot & Renne, 2003; Cui et al., 2021). In addition, contact metamorphism in the shallow plumbing systems of LIPs emplaced in sedimentary basins can generate extensive amounts of greenhouse gases (Aarnes et al., 2010), which may be subsequently released to the atmosphere through, for instance, hydrothermal venting (Svensen et al., 2004). The eruption of large igneous provinces (LIPs), and the emplacement of their subsurface plumbing systems, is often correlated with global climate change, which potentially lead to mass extinctions (Courtillot & Renne, 2003; Cui et al., 2021; Ernst & Youbi, 2017; Svensen et al., 2019).

The significant magma volumes affecting Svalbard in the Early Cretaceous have likely led to significant maturation of intruded host rocks, particularly for the organic-rich Triassic and Jurassic siliciclastic successions. The processes affecting the host rocks affected by sill emplacement are relatively well understood from other volcanic basins and include, amongst others, loss of TOC, devolatilization, compaction and density changes (Aarnes et al., 2010; Spacapan et al., 2018). Basin-scale host rock composition plays a major role in understanding how much greenhouse gasses will be released during contact metamorphism. Limestone-dominated basins, for instance, will generate an order of magnitude less CH4 and CO_2 emissions than shale-dominated basins (Aarnes, Fristad, et al., 2011). In central Spitsbergen, most of the sills are emplaced in organic-rich formations, with the Middle to Late Triassic units particularly favored by the magma. As such, we expect that significant volumes of greenhouse gasses were liberated during contact metamorphism.

Modeling is needed to quantify the amount of carbon that may have been released (e.g., Iyer et al., 2013, 2018). The challenge is that adequate data to test the models is not available. Senger, Planke, et al. (2014) use Rock-Eval

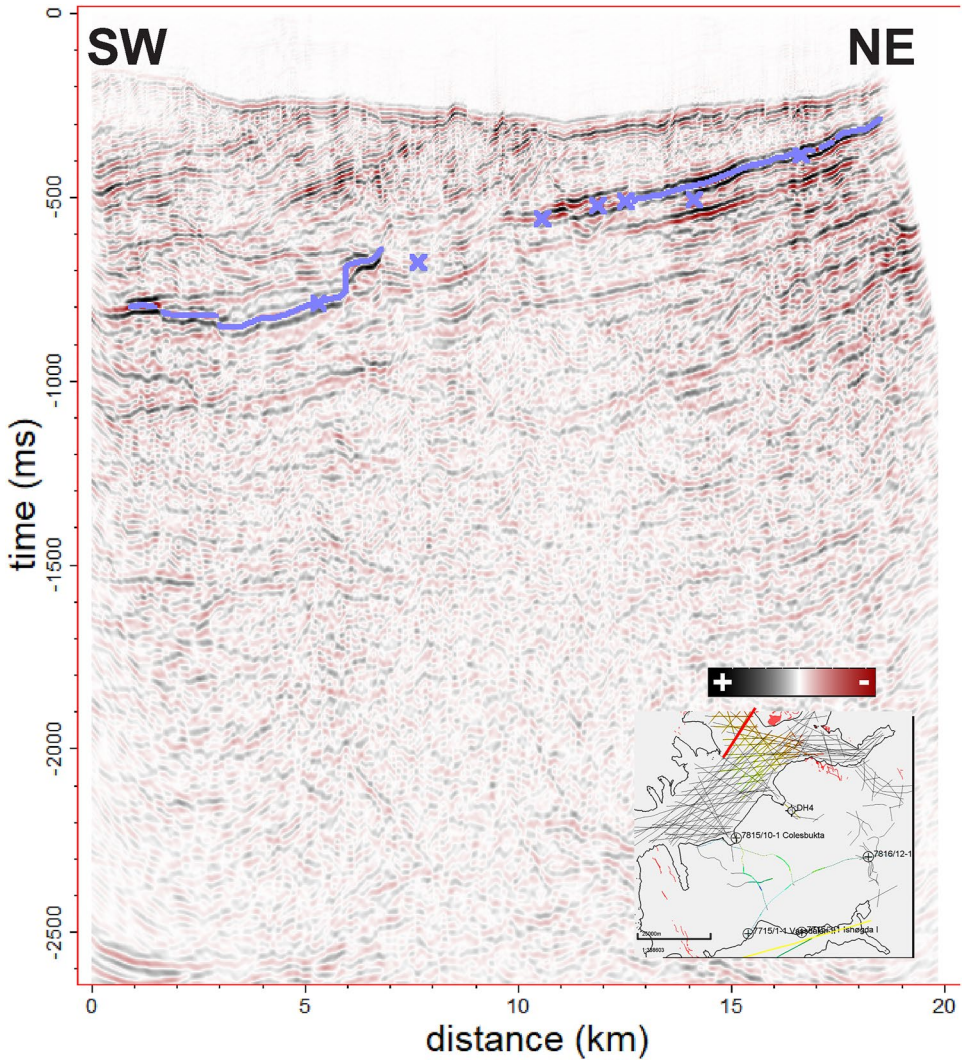

Figure 11. Offshore seismic line ST8515R87-119 in northern Isfjorden, highlighting the igneous intrusions interpreted on the 2D seismic (blue line) and the intersecting crossing lines (blue crosses).

and $\delta^{13}C$ analyses on 33 samples from the upper and lower aureole surrounding a thin (2.28 m thick) sill emplaced in relatively organic-poor (TOC < 1.5%) strata of the De Geerdalen Formation in Adventdalen, concluding that the aureole thickness is 160%–195% of the sill thickness. Hubred (2006) analyzes contact aureoles in the Botneheia Formation at five locations throughout Svalbard, including the upper aureole of a 35 m thick sill exposed along the Botneheia mountain in central Spitsbergen (see Figure 11 for location), using a range of geochemical parameters (Rock-Eval, Vitrinite). Different parameters react differently to the distance from the intrusion, with some affected already within 1.5 sill thickness distance and others only at half sill thickness. Further afield, in eastern Svalbard on south-eastern Edgeøya, Brekke et al. (2014) investigate thermally altered sections of the Botneheia Formation and conclude that over 90% of the original petroleum potential was realized through the thermal metamorphism. In this area the Mesozoic source rocks are immature and regional burial cannot explain the petroleum generation. Interestingly, the sections are not in direct contact with any igneous intrusions. A subsurface continuation of a dolerite cluster some 10 km south of the study area is postulated. Future studies must focus on high-resolution sampling of upper and lower aureoles, ideally in locations where host rock successions unaffected by contact metamorphism can also be sampled.

Further afield, Goodarzi et al. (2019) use exploration borehole data from the Sverdrup Basin in Arctic Canada to quantify the contact metamorphic aureoles around thick (45, 75, and 120 m) sills. They conclude that thermal effects of sills can be seen at distances up to 7× the sill thickness, and are controlled by sill thickness, sill spacing,

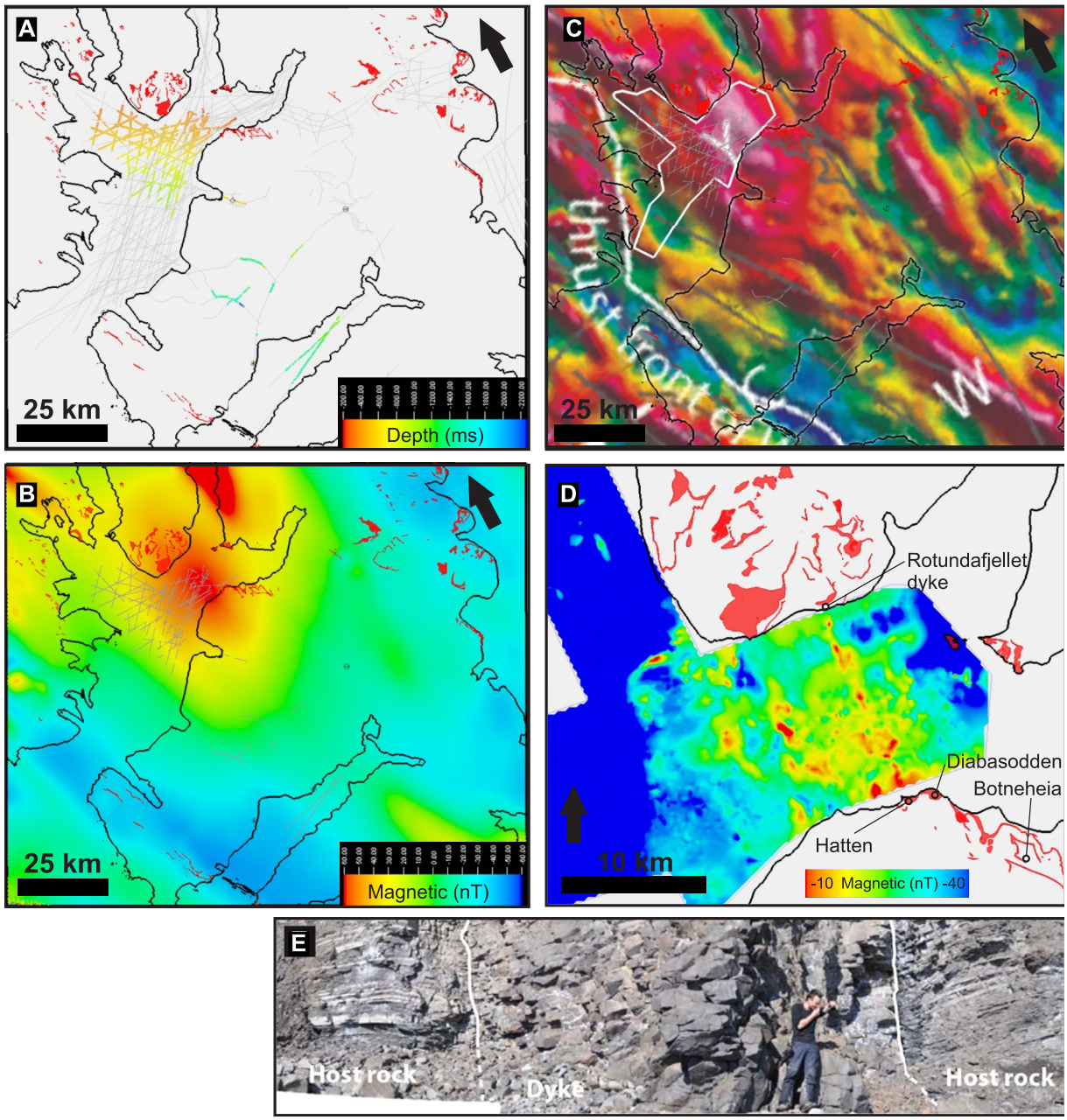

Figure 12. Integration of seismic and non-seismic data across the study area. (a) Extent and depth of igneous intrusions interpreted on 2D seismic data. The coverage of the sparse 2D seismic database is shown in gray, while igneous intrusions exposed in the field are highlighted in red. (b) Regional aeromagnetic data, with location of igneous intrusions in field (red) and interpreted on the 2D seismic data (gray) overlain. Magnetic data from NGU (Dallmann, 2015), survey details in Skilbrei (1992). (c) Magnetic anomaly map with TDR edge detection, figure from Dallmann (2015). The white polygon indicates the coverage of ship-based magnetic data shown in (d) (d) Ship-based magnetic data from Svalex, initially presented in Senger et al. (2013). (e) Field photo of the ca. 10 m thick dyke exposed at the beach beneath Rotundafjellet.

intrusion timing and pre-intrusion degree of maturation of the host rock. Goodarzi et al. (2019) also conclude that magmatic activity did not cause widespread destruction of hydrocarbons pre-dating intrusions. Jones et al. (2007) conduct 1D basin modeling and illustrate that enhanced heat flow related to HALIP magmatism contributed to enhanced hydrocarbon production in otherwise immature shallower source rocks, contributing primarily to gas production within the metamorphic aureoles.

The emplacement depth is of importance when considering the possibility that some of these generated greenhouse gasses reached the atmosphere. In addition, the emplacement depth is an important proxy for the

Geochemistry, Geophysics, Geosystems

10.1029/2021GC010300

Table 2
Overview of the Igneous Intrusions Encountered in the Exploration and Research Wells

	Intrusion				Host rock			Data availability							
Borehole	Depth to top (m MD)	Thickness (m)	Base Helvetia-fjellet Fm (m)	Emplacement depth[a] (m)	Formation	Lithology[b]	Average TOC	Core	GR[c]	RHOB	Vp	Res	CL	GC	References
DH4	950	2	188	762	De Geerdalen	sst/slst/sh	<1.5%	X	not over sill					X	Senger, Planke, et al. (2014) and Senger, Tveranger, et al. (2014)
7815/10-1 Colesbukta	2,545	43	967	1,578	Botneheia	sh	5%		X			X		X	Shkola (1977), NPD
7715/3-1 Ishøgda	2,272	6	1,329	943	De Geerdalen	sst/slst/sh	<1.5%		X		X	X			NPD
7715/3-1 Ishøgda	2,494	61	1,329	1,165	Botneheia	sh	5%		X						NPD
7715/1-1 Vassdalen II	2,211	18	1,496	715	De Geerdalen	sst/slst	<1.5%		X			X			NPD
7715/1-1 Vassdalen II	2,231	2	1,496	735	Tschermakfjellet	slst/sh	1.60%		X			X			NPD
7715/1–2 Vassdalen III	2,236	1	1,509	727	Tschermakfjellet	slst/sh	1.60%							X	Bro (2007a, 2007b), NPD
7715/1–2 Vassdalen III	2,240	4	1,509	731	Tschermakfjellet	slst/sh	1.60%							X	Bro (2007a, 2007b), NPD
7715/1–2 Vassdalen III	2,246	4	1,509	737	Tschermakfjellet	slst/sh	1.60%							X	Bro (2007a, 2007b), NPD
7816/12-1 Reindalspasset	2,213	21	354	1,859	Ebbadalen	sst	<0.5%		X	X	X		X		Norsk Hydro (1991), NPD

[a]Calculated from top of intrusion to the base of the Helvetiafjellet Formation. [b]sh, shale; slst, siltstone; sst, sandstone. [c]GR, Gamma Ray; RHOB, Density; Vp, P-velocity/sonic; Res, Resistivity; CL, Caliper; GC, geochemical data.

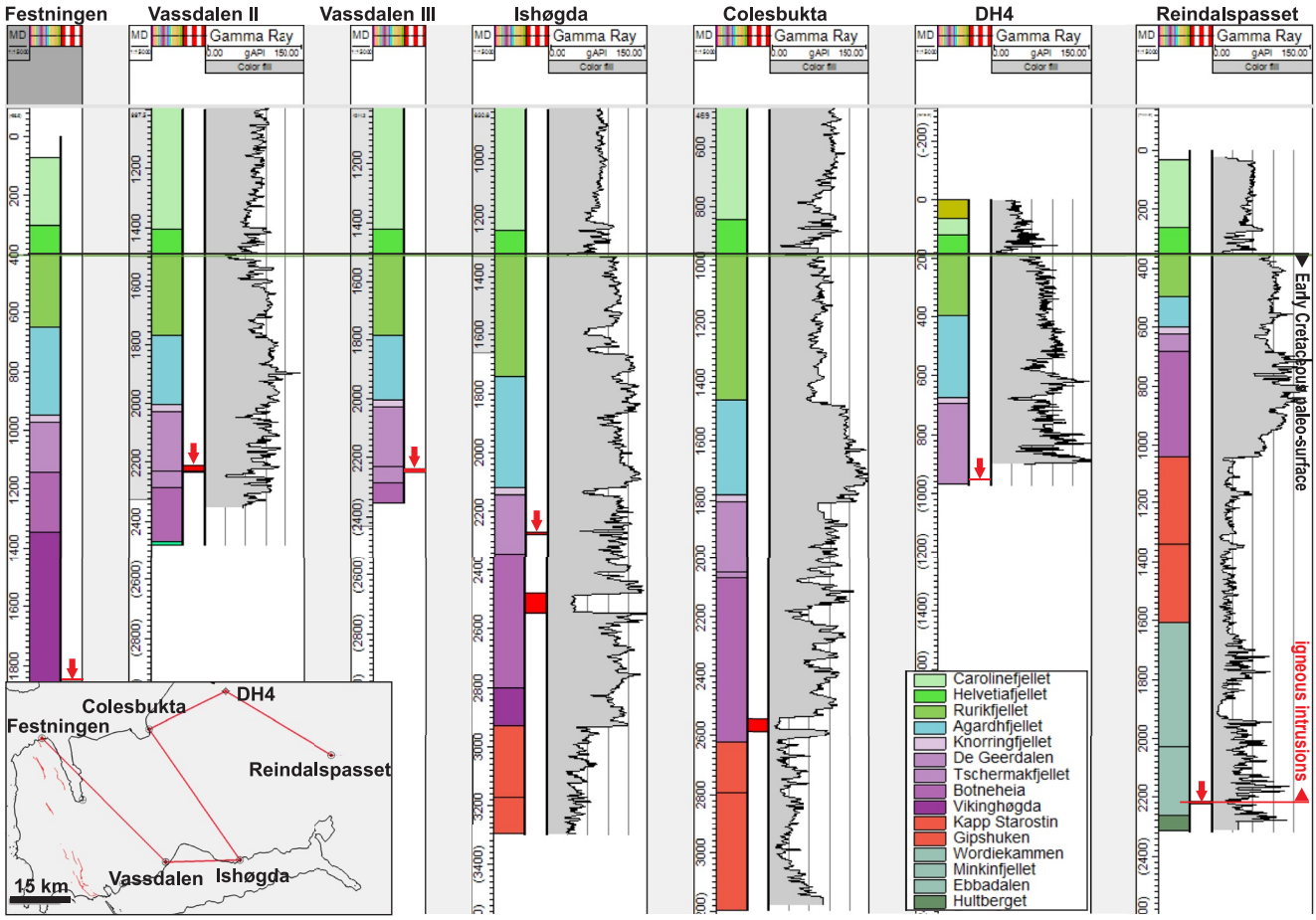

Figure 13. Overview of the regional stratigraphy in the Festningen section and onshore boreholes penetrating igneous intrusions within the Upper Paleozoic-Mesozoic succession underlying the Central Spitsbergen Basin. The stratigraphic position of the penetrated intrusions is highlighted, and the well correlation section is flattened on the base of the Helvetiafjellet Formation, that is, the paleo-surface at the time of magma emplacement. Thin intrusions are marked by a red arrow for clarity.

background host rock temperature at the time of magma emplacement, which is also a key parameter affecting the effectiveness of the contact metamorphism (Aarnes et al., 2010). Using the base of the Helvetiafjellet Formation as a paleo-surface datum, most intrusions were emplaced at <1 km beneath the surface (Table 2). The 21 m thick intrusion emplaced in the organic-poor paralic deposits in the Reindalspasset well was emplaced at ca. 1.8 km depth and would have likely not generated much greenhouse gasses anyway. The thick intrusion (43 m) at Colesbukta may have been emplaced at 1.6 km depth, but this is likely over-estimated as Paleogene thrust faults and repeated sections are present in the overburden. Overall, we foresee that the relatively shallow emplacement depth will facilitate atmospheric de-gassing. Hydrothermal vent complexes, as described from onshore the Karoo basin (Svensen et al., 2006) and 3D seismic data offshore northeast Greenland (Reynolds et al., 2017), may prove to be important conduits for the generated gasses. At present, no clear evidence exists for their occurrence in Svalbard, though Figure 9 may show a tentative vent complex and Senger et al. (2013) argue for a potential hydrothermal vent complex in Isfjorden. Fault zones, in particular the long-lived N-S trending lineaments dissecting the study area, may also act as preferential fluid migration and magma emplacement pathways.

5.3. Knowledge Gaps and Future Research Directions

While this study provides quantitative data on the spatial and stratigraphic extent of Early Cretaceous igneous intrusions in the most data-rich part of Svalbard, central Spitsbergen, it evidences fundamental knowledge gaps that pinpoint future research directions (Figure 1).

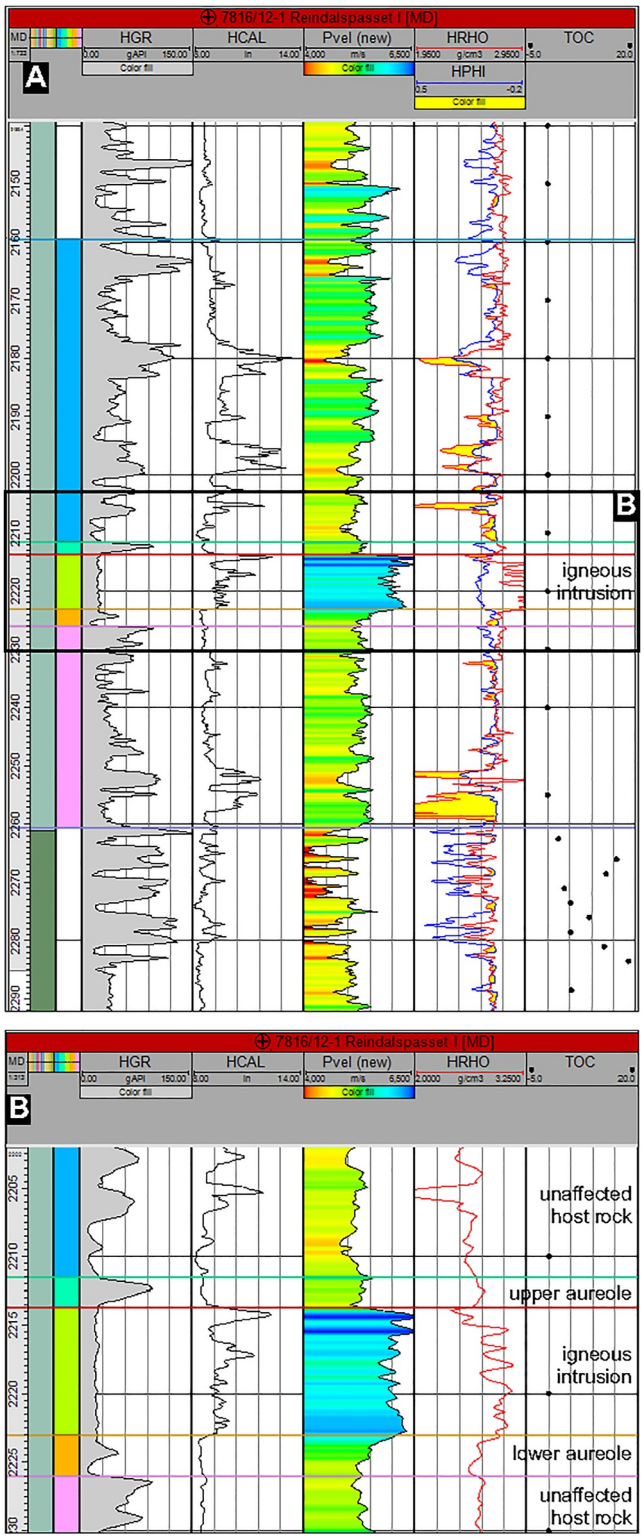

Figure 14. Characterization of the intrusion penetrated by the onshore 7816/12-1 Reindalspasset well through a wireline log suite across the intrusion and the surrounding host rock. Note the discrete log illustrating the intrusion, its upper and lower aureole and the upper and lower host rock.

Arguably the most pressing knowledge gap relates to the lack of robust geochronological data beyond the three samples presented by Corfu et al. (2013). The emplacement mechanism and timing of the HALIP are poorly constrained when compared to other known LIPs, for instance the Karoo igneous province (Svensen et al., 2012) or the Siberian Traps (Augland et al., 2019). Both of these LIPs are associated with very rapid magma emplacement across the entire basin (0.47 Myr for the Karoo province; Svensen et al., 2012). Thus, it is imperative to provide additional, regional, geochronological constraints of dykes, sills and lava flows and re-evaluate how these particular pulses may have influenced Arctic basin development and the regional-to-global environmental changes from the Early Cretaceous onwards. Comparison of HALIP magmatism in Svalbard to other HALIP provinces, in particular the Sverdrup Basin which seems to be affected by a number of pulses all of which are attributed to HALIP (Dockman et al., 2018; Kingsbury et al., 2017), is crucial to truly decipher the role that HALIP activity played in the Arctic Basin break-up.

Also of circum-Arctic relevance is the systematic collection of geochemical data from the Diabasodden Suite. At present, most of the published geochemical data sets rely on samples from relatively well-accessible coastal locations. Systematic acquisition targeting inland localities is required to expand the spatial extent of the data set. Both dolerites and host rocks should be sampled to assist in deciphering magma genesis and evolution, for instance using Sr isotopes to quantify crustal assimilation and lithospheric thickness (e.g., Hagen-Peter et al., 2019), with direct implications for quantifying magma emplaced as documented for the Sverdrup Basin by Dockman et al. (2018).

Detailed aureole studies should be undertaken to quantify how much greenhouses gases could have been liberated from the different host rocks. At present, only a handful of detailed aureole studies on outcrops are available (Brekke et al., 2014; Hubred, 2006) but are, like the aforementioned study of the DH4 borehole (Senger, Planke, et al., 2014), only addressing the Triassic shales. Detailed work, including calibrated modeling, is required to decipher the magma-fluid-rock interactions in shales, evaporites, carbonates, sandstones and basement rocks exposed throughout Svalbard.

On a regional scale, it is still not clear how magma was emplaced in Svalbard. In particular, the interaction of magma with pre-existing weakness zones like the Billefjorden Fault Zone remains unclear. Similarly, regional magma emplacement directions and mechanisms related to HALIP pulsing are unknown. For instance, conflicting models of circum-Arctic dyke emplacement are proposed, involving either a giant circumferential dyke swarm (Buchan & Ernst, 2018) or conjugate dyke swarms (Minakov et al., 2018), with direct implications on the spatial distribution of HALIP-related magma in Svalbard and its relation to crustal tectonic structures. Detailed geophysical mapping and field studies are required to further test and refine these end-member models.

The onshore-offshore extent of the HALIP rocks in Svalbard provide an excellent opportunity to directly link the "seismic-scale" outcrops with seismic data through seismic modeling (e.g., Eide et al., 2018; Rabbel et al., 2018). Geology-driven seismic modeling can provide detection thresholds of igneous intrusions in such uplifted basins to quantify how many igneous intrusions are not "seen" in the seismic data. Given the large proportion of relatively thin (<10 m) sills in both boreholes and in the field, thin sills are

10.1029/2021GC010300

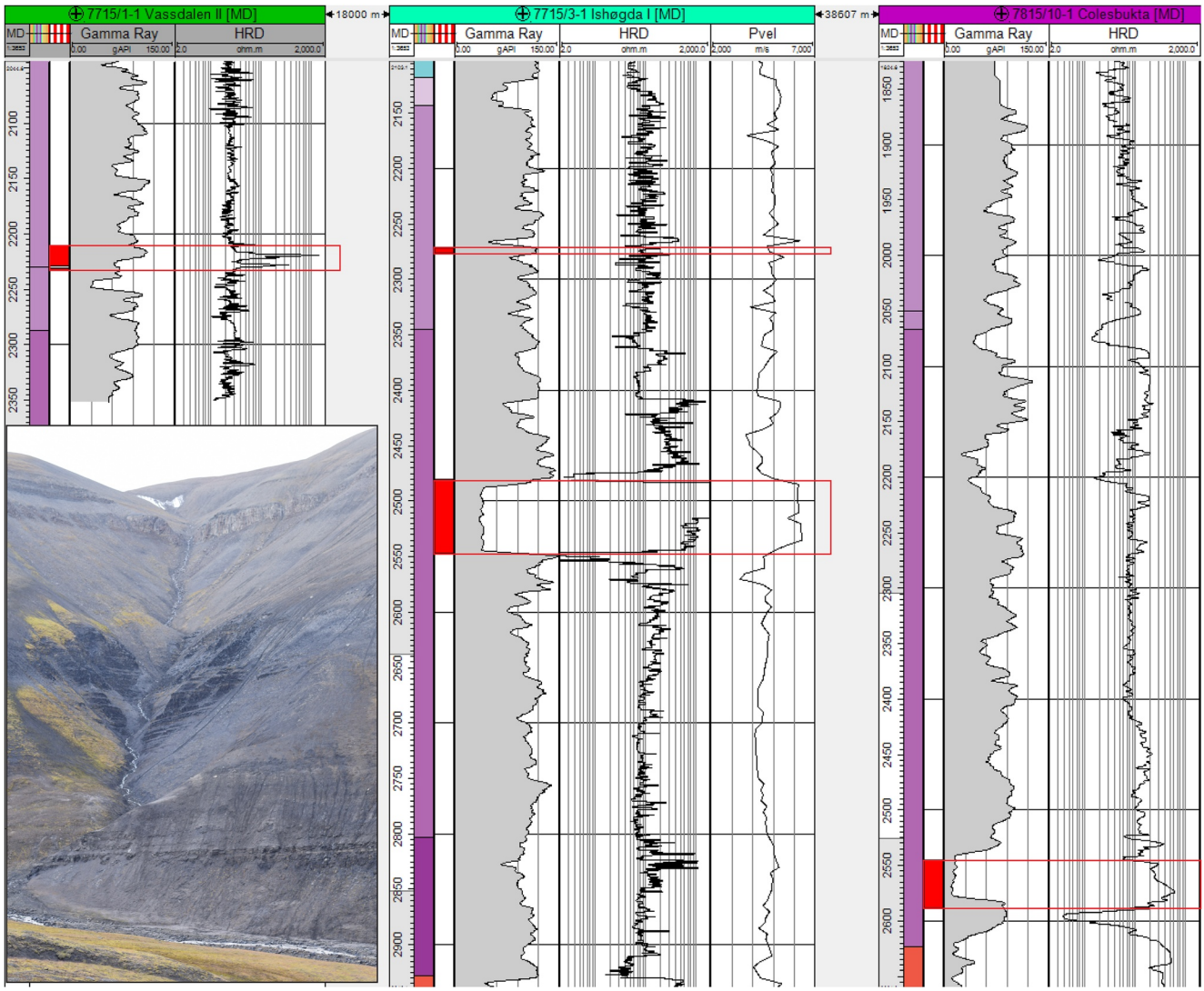

Figure 15. Well correlation across the igneous intrusions penetrated by onshore petroleum exploration boreholes in central Spitsbergen, focusing on the Triassic host rock stratigraphy. The well section is flattened on the top of the Botneheia Formation. The inset image shows the Triassic siliciclastic strata with igneous intrusions at Botneheia, the total section is approximately 250 m high.

potentially more present than what seismic data suggest. As even thin sills generate considerable aureoles (Senger et al., 2014) and stacked sills can generate substantive greenhouse gasses (Aarnes, Svensen, et al., 2011).

Considering that the Diabasodden Suite intrusions are likely the geographically most widespread geological unit in Svalbard, very few detailed field studies addressing the intrusive complex geometry have so far been undertaken. Previous field mapping in central Spitsbergen (e.g., Sartell, 2021; Senger et al., 2013) discovered suitable outcrops for addressing sill-dyke, magma-fault and magma-sediment interactions, for which quantitative detailed studies are required.

In summary, we suggest that the exceptionally exposed and relatively well-accessible Early Cretaceous igneous rocks in Svalbard finally receive the attention from multi-disciplinary research teams that they deserve. Targeted and systematic work on the Diabasodden Suite will not only contribute to elucidating some of the remaining knowledge gaps related to the HALIP (e.g., geochronology), but also provide generic knowledge on how magmatism affects the paleo-environment through contact metamorphism in variable host rocks.

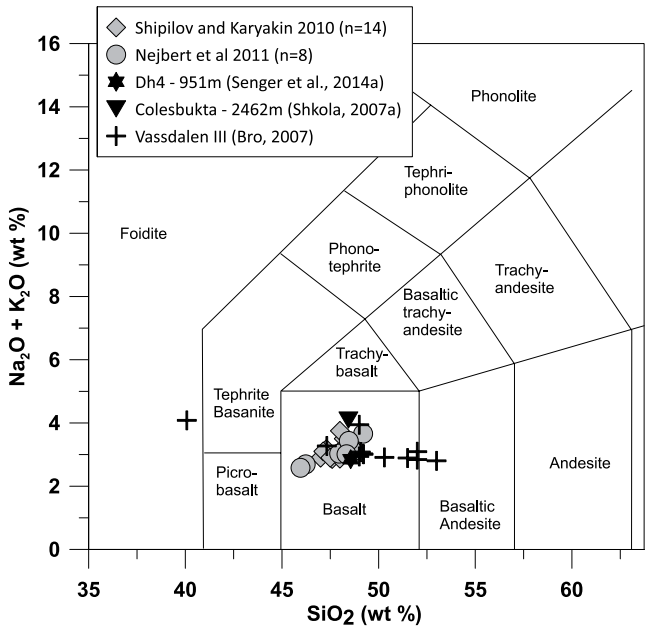

Figure 16. Silica versus total alkalis plot, following Bas et al. (1986), comparing the geochemical signature of the dolerite intrusions penetrated by the Dh4 (Senger, Planke, et al., 2014), Vassdalen III (Bro, 2007c) and Colesbukta (Shkola, 2007) boreholes and with published geochemical data to the Diabasodden Suite dolerites outcrops (Nejbert et al., 2011; Shipilov & Karyakin, 2011). Note the clear basaltic affinity of the borehole samples compared to published Diabasodden Suite rocks.

6. Conclusions

In this study, we have integrated all available data to quantify the spatial and stratigraphic extent of Early Cretaceous igneous intrusions in central Spitsbergen. We conclude that:

- Igneous intrusions are widespread in central Spitsbergen, with 265 individual intrusions within the study area. They are directly exposed over an area of 72 km^2 (1.6% of the entire study area) and are inferred from seismic data over an area of 3,000 km^2. These represent a magma volume of 0.14–2.52 km^3 and 3.2–195.2 km^3, respectively.
- Igneous intrusions are emplaced in Carboniferous to Jurassic host rocks. Most intrusions occur in organic-rich mudstones (of Middle Triassic and Late Jurassic age) and in Permian spiculites.
- Five petroleum exploration boreholes in the study area penetrate igneous intrusions. Wireline data are used to characterize the sills and associated contact metamorphic aureoles. Sills exhibit high velocity and resistivity and low gamma ray. Aureoles are present in particular in organic-rich shales and are characterized by very low resistivity and an increasing velocity toward the sill.
- Ship-based magnetic data provide a direct link from the onshore outcrops. A 10 m dyke exposed on the beach can be followed for >15 km beneath Isfjorden as a high magnetic anomaly.
- Previously unpublished geochemical data from drilled intrusions in Colesbukta and Vassdalen indicate that these have the same basaltic composition as exposed Diabasodden Suite dolerites.

With this work, we aim at showing that Svalbard offers a unique environment to study HALIP magmatism. We foresee that this work in the most data-rich part of Svalbard will facilitate future integrated work on the Svalbard dolerites. We thus provide an overview of the identified knowledge gaps that will improve our understanding of HALIP magmatism in Svalbard.

Table 3
Comparison of Our Results With Key Published Estimates From Svalbard and Other High Arctic Large Igneous Province (HALIP) Provinces

Study area	Magma area (km^2)	Sill thickness (m)	Magma volume (km^3)	Timing and duration	References
Central Spitsbergen (field)	72	2–35 m	0.14–2.52	-	This study
Central Spitsbergen (subsurface)	3,200	1–61 m (avg 16.2)	3.2–195.2 (avg 51.84)	-	This study
Svalbard	120,000	10–50	1,200-6,000	-	This study
Svalbard	-	50-100 (cum.)	>10,000	135–90 Ma	Maher (2001)
Ekmanfjorden, Svalbard	-	-	0.25–0.52	-	Sartell (2021)
Barents Shelf (including Svalbard)	900,000	114-228 (cum.)	200,000	125–122 Ma	Polteau et al. (2016)
Svalbard area	200,000	50	10,000	-	Grogan et al. (2000)
Svalbard	-	-	-	124.5 Ma	Corfu et al. (2013)
Franz Josef Land	-	80–100	>20,000	140–90 Ma	Maher (2001)
Sverdrup Basin	30,000	300 (cum.)	>100,000	-	Saumur et al. (2016)
Sverdrup Basin	-	-	-	3 pulses: 124–120 Ma 99–91 Ma 85–77 Ma	Dockman et al. (2018)
Alpha-Mendeleev Ridge	13,000 000	-	~200,000,000	-	Oakey and Saltus (2016)
HALIP	-	-	-	130–80 Ma	Bryan and Ernst (2008)

Data Availability Statement

Archive and exploration well data is available in data repositories such as Zenodo (Senger et al., 2022) and Pangaea (Bro, 2007c; Shkola, 2007). Vintage seismic data from the 1980s and 1990s is described in the cited literature (Bælum et al., 2012; Blinova et al., 2013; Senger et al., 2013) and full-stack lines are available at UNIS.

Acknowledgments
We are indebted to many stimulating discussions on the Svalbard dolerites with, amongst others, Ole Rabbel, Sverre Planke, Anna Sartell, Kei Ogata, Snorre Olaussen, Alvar Braathen and Jan Tveranger. Specific assistance to this manuscript was provided by Peter Betlem who provided a script for quantitatively analyzing GIS data and Aleksandra Smyrak-Sikora who carefully proof-read the manuscript. This project has been partly funded by the Research Centre for Arctic Petroleum Exploration (ARCEx; www.arcex.no), The University Centre in Svalbard (UNIS) an Arctic Field Grant from the Svalbard Science Forum and the NORRAM2 collaboration project led by CEED/UiO (https://norramarctic.wordpress.com/). UNIS sincerely appreciates academic licenses of Petrel, the Blueback Petrel plug-ins and Metashape from Schlumberger, Cegal and Agisoft respectively. Exploration well data were kindly provided by the Norwegian Petroleum Directorate, Equinor (Reindalspasset borehole) and Norsk Polar Navigasjon, research borehole data were provided by the UNIS CO_2 lab project (http://co2-ccs.unis.no) and geological and terrain model data were provided by the Norwegian Polar Institute (http://geodata.npolar.no). The Czech Arctic Research Station and UNIS logistics facilitated numerous field campaigns targeting the Svalbard dolerites in the past years. Finally, we sincerely appreciate the constructive comments from two anonymous journal reviewers.

References

Aarnes, I., Fristad, K., Planke, S., & Svensen, H. (2011). The impact of host-rock composition on devolatilization of sedimentary rocks during contact metamorphism around mafic sheet intrusions. *Geochemistry, Geophysics, Geosystems*, *12*(10), Q10019. https://doi.org/10.1029/2011gc003636

Aarnes, I., Svensen, H., Connolly, J. A. D., & Podladchikov, Y. Y. (2010). How contact metamorphism can trigger global climate changes: Modeling gas generation around igneous sills in sedimentary basins. *Geochimica et Cosmochimica Acta*, *74*(24), 7179–7195. https://doi.org/10.1016/j.gca.2010.09.011

Aarnes, I., Svensen, H., Polteau, S., & Planke, S. (2011). Contact metamorphic devolatilization of shales in the Karoo Basin, South Africa, and the effects of multiple sill intrusions. *Chemical Geology*, *281*(3–4), 181–194. https://doi.org/10.1016/j.chemgeo.2010.12.007

Anell, I., Braathen, A., & Olaussen, S. (2014). The Triassic-Early Jurassic of the northern Barents Shelf: A regional understanding of the Longyearbyen CO_2 reservoir. *Norwegian Journal of Geology*, *94*(2–3), 83–98.

Augland, L., Ryabov, V., Vernikovsky, V., Planke, S., Polozov, A., Callegaro, S., et al. (2019). The main pulse of the Siberian Traps expanded in size and composition. *Scientific Reports*, *9*(1), 1–12. https://doi.org/10.1038/s41598-019-54023-2

Bailey, J. C., & Rasmussen, M. H. (1997). Petrochemistry of Jurassic and Cretaceous tholeiites from Kong Karls Land, Svalbard, and their relation to Mesozoic magmatism in the Arctic. *Polar Research*, *16*(1), 37–62. https://doi.org/10.1111/j.1751-8369.1997.tb00726.x

Bælum, K., & Braathen, A. (2012). Along-strike changes in fault array and rift basin geometry of the Carboniferous Billefjorden Trough, Svalbard, Norway. *Tectonophysics*, *546–547*, 38–55. https://doi.org/10.1016/j.tecto.2012.04.009

Bælum, K., Johansen, T. A., Johnsen, H., Rød, K., Ruud, B. O., & Braathen, A. (2012). Subsurface geometries of the Longyearbyen CO2 lab in Central Spitsbergen, as mapped by reflection seismic data. *Norwegian Journal of Geology*, *92*, 377–389.

Bas, M. J., Maitre, R. W., Streckeisen, A., Zanettin, B., & IUGS Subcommission on the Systematics of Igneous Rocks. (1986). A chemical classification of volcanic rocks based on the total alkali-silica diagram. *Journal of Petrology*, *27*(3), 745–750. https://doi.org/10.1093/petrology/27.3.745

Bédard, J. H., Troll, V. R., Deegan, F. M., Tegner, C., Saumur, B. M., Evenchick, C. A., et al. (2021). High Arctic Large Igneous Province alkaline rocks in Canada: Evidence for multiple mantle components. *Journal of Petrology*, *62*(9), egab042. https://doi.org/10.1093/petrology/egab042

Bergh, S. G., Braathen, A., & Andresen, A. (1997). Interaction of basement-involved and thin-skinned tectonism in the Tertiary fold-thrust belt of central Spitsbergen, Svalbard. *American Association of Petroleum Geologists Bulletin*, *81*(4), 637–661.

Birkenmajer, K., Krajewski, K. P., Pécskay, Z., & Lorenc, M. W. (2010). K−Ar dating of basic intrusions at Bellsund, Spitsbergen, Svalbard. *Polish Polar Research*, *31*(1), 3–16. https://doi.org/10.4202/ppres.2010.01

Birkenmajer, K., & Morawski, T. (1960). Dolerite intrusions of Wedel-Jarlsberg Land, Vestspitsbergen. *Studia Geologica Polonica, IV (Geological results of the Polish 1957–1958 Spitsbergen Expedition)* (pp. 103–123).

Blinova, M., Faleide, J. I., Gabrielsen, R. H., & Mjelde, R. (2013). Analysis of structural trends of sub-sea-floor strata in the Isfjorden area of the West Spitsbergen Fold-and-Thrust Belt based on multichannel seismic data. *Journal of the Geological Society*, *170*(4), 657–668. https://doi.org/10.1144/jgs2012-109

Blomeier, D., Dustira, A. M., Forke, H., & Scheibner, C. (2013). Facies analysis and depositional environments of a storm-dominated, temperate to cold, mixed siliceous-carbonate ramp: The Permian Kapp Starostin Formation in NE Svalbard. *Norwegian Journal of Geology*, *93*(2), 75–93.

Blomeier, D., Scheibner, C., & Forke, H. (2009). Facies arrangement and cyclostratigraphic architecture of a shallow-marine, warm-water carbonate platform: The Late Carboniferous Ny Friesland platform in eastern Spitsbergen (Pyefjellet Beds, Wordiekammen Formation, Gipsdalen Group). *Facies*, *55*(2), 291–324. https://doi.org/10.1007/s10347-008-0163-3

Bond, D. P., Wignall, P. B., Keller, G., & Kerr, A. (2014). Large igneous provinces and mass extinctions: An update. *Volcanism, Impacts, and Mass Extinctions: Causes and Effects*, *505*, 29–55.

Braathen, A., Bælum, K., Christiansen, H. H., Dahl, T., Eiken, O., Elvebakk, H., et al. (2012). Longyearbyen CO2 lab of Svalbard, Norway – First assessment of the sedimentary succession for CO_2 storage. *Norwegian Journal of Geology*, *92*, 353–376.

Braathen, A., Osmundsen, P. T., Maher, H., & Ganerød, M. (2018). The Keisarhjelmen detachment records Silurian–Devonian extensional collapse in Northern Svalbard. *Terra Nova*, *30*(1), 34–39. https://doi.org/10.1111/ter.12305

Brekke, T., Krajewski, K. P., & Hubred, J. H. (2014). Organic geochemistry and petrography of thermally altered sections of the Middle Triassic Botneheia Formation on south-western Edgeøya, Svalbard. *Norwegian Petroleum Directorate Bulletin*, *11*, 111–128.

Bro, E. G. (2007a). Chemical composition of rocks from hole Vassdalensk-3 drilled in the west Svalbard. In E. G. Bro (Ed.), (1990): *Processing results from parametric drill hole Vassdalenskaya-3, Svalbard Archipelago, north side of Van-Meyen Fjord (Report 6593, Leningrad)*. All-Russian Research Institute for Geology and Mineral Resources of the World Ocean, PANGAEA. https://doi.org/10.1594/PANGAEA.615278

Bro, E. G. (2007b). Physical properties of rocks from hole Vassdalensk-2 drilled in the west Svalbard. In E. G. Bro (Ed.), (1990): *Processing results from parametric drill hole Vassdalenskaya-2, Svalbard Archipelago, north side of Van-Meyen Fjord (Report 6593, Leningrad)*. All-Russian Research Institute for Geology and Mineral Resources of the World Ocean, PANGAEA. https://doi.org/10.1594/PANGAEA.619100

Bro, E. G. (2007c). Physical properties of rocks from hole Vassdalensk-3 drilled in the west Svalbard. In E. G. Bro (Ed.), (1990): *Processing results from parametric drill hole Vassdalenskaya-3, Svalbard Archipelago, north side of Van-Meyen Fjord (Report 6593, Leningrad)*. All-Russian Research Institute for Geology and Mineral Resources of the World Ocean, PANGAEA. https://doi.org/10.1594/PANGAEA.619101

Bryan, S. E., & Ernst, R. E. (2008). Revised definition of large igneous provinces (LIPs). *Earth-Science Reviews*, *86*(1–4), 175–202. https://doi.org/10.1016/j.earscirev.2007.08.008

Buchan, K. L., & Ernst, R. E. (2018). A giant circumferential dyke swarm associated with the High Arctic Large Igneous Province (HALIP). *Gondwana Research*, *58*, 39–57. https://doi.org/10.1016/j.gr.2018.02.006

Burgess, S. D., Muirhead, J. D., & Bowring, S. A. (2017). Initial pulse of Siberian Traps sills as the trigger of the end-Permian mass extinction. *Nature Communications*, *8*(1), 1–6. https://doi.org/10.1038/s41467-017-00083-9

Burov, P., Krasil'scikov, A. A., Firsov, L. V., & Klubov, B. A. (1977). The age of Spitsbergen Dolerites (from isotopic dating). *Norsk Polarinstitutt Arbok*, *1975*, 101–108.

Corfu, F., Polteau, S., Planke, S., Faleide, J. I., Svensen, H., Zayoncheck, A., & Stolbov, N. (2013). U-Pb geochronology of Cretaceous magmatism on Svalbard and Franz Josef Land, Barents Sea large igneous province. *Geological Magazine*, *150*(6), 1–9. https://doi.org/10.1017/S0016756813000162

Courtillot, V. E., & Renne, P. R. (2003). On the ages of flood basalt events. *Comptes Rendus Geoscience*, *335*(1), 113–140. https://doi.org/10.1016/s1631-0713(03)00006-3

Cui, Y., Li, M., van Soelen, E. E., Peterse, F., & Kürschner, W. M. (2021). Massive and rapid predominantly volcanic CO_2 emission during the end-Permian mass extinction. *Proceedings of the National Academy of Sciences*, *118*(37), 1–11. https://doi.org/10.1073/pnas.2014701118

Dallmann, W. (2015). Geoscience Atlas of Svalbard. *Norsk Polarinstitutt Rapportserie*, *148*, 292.

Dallmann, W. K., Dypvik, H., Gjelberg, J. G., Harland, W. B., Johannessen, E. P., Keilen, H. B., et al. (1999). *Lithostratigraphic Lexicon of Svalbard: Review and recommendations for nomenclature use* (p. 318). Norsk Polarinstitutt.

de Miranda, F. S., Vettorazzi, A. L., da Cruz Cunha, P. R., Aragão, F. B., Michelon, D., Caldeira, J. L., et al. (2018). Atypical igneous-sedimentary petroleum systems of the Parnaíba Basin, Brazil: Seismic, well logs and cores. *Geological Society, London, Special Publications*, *472*(1), 341–360. https://doi.org/10.1144/sp472.15

Dibner, V. (1998). Geology of Franz Josef Land. *Norsk Polarinstitutt Meddelelser nr*, *146*, 190.

Dockman, D., Pearson, D., Heaman, L., Gibson, S., & Sarkar, C. (2018). Timing and origin of magmatism in the Sverdrup Basin, Northern Canada—Implications for lithospheric evolution in the High Arctic Large Igneous Province (HALIP). *Tectonophysics*, *742*, 50–65. https://doi.org/10.1016/j.tecto.2018.05.010

Døssing, A., Jackson, H. R., Matzka, J., Einarsson, I., Rasmussen, T. M., Olesen, A. V., & Brozena, J. M. (2013). On the origin of the Amerasia Basin and the High Arctic Large Igneous Province—Results of new aeromagnetic data. *Earth and Planetary Science Letters*, *363*, 219–230. https://doi.org/10.1016/j.epsl.2012.12.013

Eide, C. H., Schofield, N., Lecomte, I., Buckley, S. J., & Howell, J. A. (2018). Seismic interpretation of sill complexes in sedimentary basins: Implications for the sub-sill imaging problem. *Journal of the Geological Society*, *175*(2), 193–209. https://doi.org/10.1144/jgs2017-096

Eiken, O., Degutsch, M., Riste, P., & Rød, K. (1989). Snowstreamer: An efficient tool in seismic acquisition. *First Break*, *7*(9), 374–378. https://doi.org/10.3997/1365-2397.1989021

Ernst, R. E., & Youbi, N. (2017). How Large Igneous Provinces affect global climate, sometimes cause mass extinctions, and represent natural markers in the geological record. *Palaeogeography, Palaeoclimatology, Palaeoecology*, *478*, 30–52. https://doi.org/10.1016/j.palaeo.2017.03.014

Evenchick, C. A., Davis, W. J., Bédard, J. H., Hayward, N., & Friedman, R. M. (2015). Evidence for protracted High Arctic large igneous province magmatism in the central Sverdrup Basin from stratigraphy, geochronology, and paleodepths of saucer-shaped sills. *GSA Bulletin*, *127*(9–10), 1366–1390. https://doi.org/10.1130/b31190.1

Firshov, L. V., & Livshits (1967). Potassium-Argon dating of dolerites from the region of Sassenfjorden (in Russian). In V. N. Sokolov (Ed.), *Materialy po stratigrafii Spicbergena* (pp. 178–184). Institut Geologii Arktiki.

Gayer, R. A., Gee, D. G., Winsnes, T. S., Harland, W. B., Wallis, R. H., Miller, J. A., & Spall, H. R. (1966). Radiometric age determinations on rocks from Spitsbergen. *Norsk Polarinstitutt Skrifter*, *137*, 4–39.

Gee, D. G., & Tebenkov, A. M. (2004). Svalbard: A fragment of the Laurentian margin. *Geological Society, London, Memoirs*, *30*(1), 191–206. https://doi.org/10.1144/gsl.mem.2004.030.01.16

Geissler, W. H., Estrada, S., Riefstahl, F., O'Connor, J. M., Spiegel, C., Van den Boogard, P., & Klügel, A. (2019). Middle Miocene magmatic activity in the Sophia Basin, Arctic Ocean—Evidence from dredged basalt at the flanks of Mosby Seamount. *Arktos*, *5*(1), 31–48. https://doi.org/10.1007/s41063-019-00066-8

Goodarzi, F., Gentzis, T., & Dewing, K. (2019). Influence of igneous intrusions on the thermal maturity of organic matter in the Sverdrup Basin, Arctic Canada. *International Journal of Coal Geology*, *213*, 103280. https://doi.org/10.1016/j.coal.2019.103280

Grégoire, M., Chevet, J., & Maaloe, S. (2010). Composite xenoliths from Spitsbergen: Evidence of the circulation of MORB-related melts within the upper mantle. *Geological Society, London, Special Publications*, *337*(1), 71–86. https://doi.org/10.1144/sp337.4

Grogan, P., Nyberg, K., Fotland, B., Myklebust, R., Dahlgren, S., & Riis, F. (2000). Cretaceous magmatism south and east of Svalbard: Evidence from seismic reflection and magnetic data. *Polarforschung*, *68*, 25–34.

Grundvåg, S.-A., Marin, D., Kairanov, B., Śliwińska, K., Nøhr-Hansen, H., Escalona, A., & Olaussen, S. (2017). The Lower Cretaceous succession of the northwestern Barents Shelf: Onshore and offshore correlations. *Marine and Petroleum Geology*, *86*, 834–857. https://doi.org/10.1016/j.marpetgeo.2017.06.036

Hagen-Peter, G., Tegner, C., & Lesher, C. E. (2019). Strontium isotope systematics for plagioclase of the Skaergaard intrusion (East Greenland): A window to crustal assimilation, differentiation, and magma dynamics. *Geology*, *47*(4), 313–316. https://doi.org/10.1130/g45639.1

Helland-Hansen, W., & Grundvåg, S. A. (2020). The Svalbard Eocene-Oligocene (?) Central Basin succession: Sedimentation patterns and controls. *Basin Research*, *33*(1), 729–753. https://doi.org/10.1111/bre.12492

Hubred, J. H. (2006). *Thermal effects of basaltic sill emplacement in source rocks on maturation and hydrocarbon generation* (Unpublished MSc Thesis), (p. 303). University of Oslo.

Ineson, J. R., Hovikoski, J., Sheldon, E., Piasecki, S., Alsen, P., Fyhn, M. B., et al. (2021). Regional impact of Early Cretaceous tectono-magmatic uplift in the Arctic: Implications of new data from eastern North Greenland. *Terra Nova*, *33*(3), 284–292. https://doi.org/10.1111/ter.12514

Iyer, K., Rüpke, L., & Galerne, C. Y. (2013). Modeling fluid flow in sedimentary basins with sill intrusions: Implications for hydrothermal venting and climate change. *Geochemistry, Geophysics, Geosystems*, *14*(12), 5244–5262. https://doi.org/10.1002/2013gc005012

Iyer, K., Svensen, H., & Schmid, D. W. (2018). SILLi 1.0: A 1-D numerical tool quantifying the thermal effects of sill intrusions. *Geoscientific Model Development*, *11*(1), 43–60. https://doi.org/10.5194/gmd-11-43-2018

Johansen, T. A., Ruud, B. O., Bakke, N. E., Riste, P., Johannessen, E. P., & Henningsen, T. (2011). Seismic profiling on Arctic glaciers. *First Break*, *29*(2), 7. https://doi.org/10.3997/1365-2397.20112st1

Jones, S., Wielens, H., Williamson, M. C., & Zentilli, M. (2007). Impact of magmatism on petroleum systems in the Sverdrup Basin, Canadian Arctic Islands, Nunavut: A numerical modelling study. *Journal of Petroleum Geology*, *30*(3), 237–256. https://doi.org/10.1111/j.1747-5457.2007.00237.x

Jowitt, S. M., Williamson, M.-C., & Ernst, R. E. (2014). Geochemistry of the 130 to 80 Ma Canadian High Arctic Large Igneous Province (HALIP) event and implications for Ni-Cu-PGE prospectivity. *Economic Geology*, *109*(2), 281–307. https://doi.org/10.2113/econgeo.109.2.281

Kingsbury, C. G., Ernst, R. E., Cousens, B. L., & Williamson, M.-C. (2016). The High Arctic LIP in Canada: Trace element and Sm-Nd isotopic evidence for the role of mantle heterogeneity and crustal assimilation. *Norwegian Journal of Geology/Norsk Geologisk Forening*, *96*(2). https://doi.org/10.17850/njg96-2-02

Kingsbury, C. G., Kamo, S. L., Ernst, R. E., Söderlund, U., & Cousens, B. L. (2017). U-Pb geochronology of the plumbing system associated with the Late Cretaceous Strand Fiord Formation, Axel Heiberg Island, Canada: Part of the 130–90 Ma high Arctic large igneous province. *Journal of Geodynamics*, *118*, 106–117. https://doi.org/10.1016/j.jog.2017.11.001

Koevoets, M. J., Hammer, Ø., Olaussen, S., Senger, K., & Smelror, M. (2018). Integrating subsurface and outcrop data of the Middle Jurassic to Lower Cretaceous Agardfjellet Formation in central Spitsbergen. *Norwegian Journal of Geology*, *98*(1), 1–34. https://doi.org/10.17850/njg98-4-01

Krajewski, K. P. (2013). Organic matter–apatite–pyrite relationships in the Botneheia Formation (Middle Triassic) of eastern Svalbard: Relevance to the formation of petroleum source rocks in the NW Barents Sea shelf. *Marine and Petroleum Geology*, *45*, 69–105. https://doi.org/10.1016/j.marpetgeo.2013.04.016

Lasabuda, A. P., Johansen, N. S., Laberg, J. S., Faleide, J. I., Senger, K., Rydningen, T. A., et al. (2021). Cenozoic uplift and erosion on the Norwegian Barents Shelf–A review. *Earth-Science Reviews*, *217*, 103609. https://doi.org/10.1016/j.earscirev.2021.103609

Li, M., Grasby, S. E., Wang, S.-J., Zhang, X., Wasylenki, L. E., Xu, Y., et al. (2021). Nickel isotopes link Siberian Traps aerosol particles to the end-Permian mass extinction. *Nature Communications*, *12*(1), 1–7. https://doi.org/10.1038/s41467-021-22066-7

Lu, Y., Li, C.-F., Wang, J., & Wan, X. (2022). Arctic geothermal structures inferred from Curie-point depths and their geodynamic implications. *Tectonophysics*, *822*, 229158. https://doi.org/10.1016/j.tecto.2021.229158

Maher, H. D., Jr. (2001). Manifestations of the Cretaceous High Arctic large igneous province in Svalbard. *The Journal of Geology*, *109*(1), 91–104. https://doi.org/10.1086/317960

Minakov, A. (2018). Late Cenozoic lithosphere dynamics in Svalbard: Interplay of glaciation, seafloor spreading and mantle convection. *Journal of Geodynamics*, *122*, 1–16. https://doi.org/10.1016/j.jog.2018.09.009

Minakov, A., Yarushina, V., Faleide, J. I., Krupnova, N., Sakoulina, T., Dergunov, N., & Glebovsky, V. (2018). Dyke emplacement and crustal structure within a continental large igneous province, northern Barents Sea. In V. Pease & B. Coakley (Eds.), *Circum-Arctic lithosphere evolution* (pp. 371–395). Geological Society. https://doi.org/10.1144/SP460.4

Mulrooney, M. J., Larsen, L., Stappen, J. V., Cnudde, V., Senger, K., Rismyhr, B., et al. (2019). Fluid flow properties of the Wilhelmøya Subgroup, a potential unconventional CO_2 storage unit in central Spitsbergen. *Norwegian Journal of Geology*, *99*, 85–116. https://doi.org/10.17850/njg002

Nejbert, K., Krajewski, K. P., Dubińska, E., & Pécskay, Z. (2011). Dolerites of Svalbard, north-west Barents Sea Shelf: Age, tectonic setting and significance for geotectonic interpretation of the High-Arctic Large Igneous Province. *Polar Research*, *30*(7306), 1–24. https://doi.org/10.3402/polar.v30i0.7306

Norsk Hydro. (1991). Final well report - 7816/12-1 Reindalspasset I.

Norwegian Polar Institute. (2014a). Geological and topographic data from Svalbard: Geodata.npolar.no. https://doi.org/10.21334/npolar.2014.dce53a47

Norwegian Polar Institute. (2014b). Terrengmodell Svalbard (S0 Terrengmodell). https://doi.org/10.21334/npolar.2014.dce53a47

Oakey, G., & Saltus, R. (2016). Geophysical analysis of the Alpha–Mendeleev ridge complex: Characterization of the High Arctic Large Igneous Province. *Tectonophysics*, *691*, 65–84. https://doi.org/10.1016/j.tecto.2016.08.005

Ogata, K., Senger, K., Braathen, A., Tveranger, J., & Olaussen, S. (2012). The importance of natural fractures in a tight reservoir for potential CO_2 storage: Case study of the upper Triassic to middle Jurassic Kapp Toscana Group (Spitsbergen, Arctic Norway). In G. H. Spence, J. Redfern, R. Aguilera, T. G. Bevan, J. W. Cosgrove, G. D. Couples, et al. (Eds.), *Advances in the study of fractured reservoirs* (p. 22). Geological Society of London. https://doi.org/10.1144/SP374.9

Olaussen, S., Grundvåg, S.-A., Senger, K., Anell, I., Betlem, P., Birchall, T., et al. (2023). *The Svalbard Carboniferous to Cenozoic composite tectono-stratigraphic element*. Geological Society of London Memoirs. https://doi.org/10.1144/M57-2021-36

Olaussen, S., Larssen, G., Helland-Hansen, W., Johannessen, E., Nøttvedt, A., Riis, F., et al. (2018). Mesozoic strata of Kong Karls Land, Svalbard, Norway; a link to the northern Barents Sea basins and platforms. *Norwegian Journal of Geology*, *98*(4), 1–69. https://doi.org/10.17850/njg98-4-06

Olaussen, S., Senger, K., Braathen, A., Grundvåg, S. A., & Mørk, A. (2019). You learn as long as you drill; research synthesis from the Longyearbyen CO_2 Laboratory, Svalbard, Norway. *Norwegian Journal of Geology*, *99*, 157–187. https://doi.org/10.17850/njg008

Piepjohn, K. (2000). The Svalbardian-Ellesmerian deformation of the Old Red Sandstone and the pre-Devonian basement in NW Spitsbergen (Svalbard). *Geological Society, London, Special Publications*, *180*(1), 585–601. https://doi.org/10.1144/gsl.sp.2000.180.01.31

Planke, S., Rasmussen, T., Rey, S. S., & Myklebust, R. (2005). *Seismic characteristics and distribution of volcanic intrusions and hydrothermal vent complexes in the Vøring and Møre basins*. *Geological Society, London, Petroleum Geology Conference Series* (pp. 833–844). Geological Society of London.

Polteau, S., Hendriks, B. W., Planke, S., Ganerød, M., Corfu, F., Faleide, J. I., et al. (2016). The Early Cretaceous Barents Sea Sill complex: Distribution, $^{40}Ar/^{39}Ar$ geochronology, and implications for carbon gas formation. *Palaeogeography, Palaeoclimatology, Palaeoecology*, *441*, 83–95. https://doi.org/10.1016/j.palaeo.2015.07.007

Prestvik, T. (1978). Cenozoic plateau lavas of Spitsbergen - A geochemical study. *Norsk Polarinstitutt Arbok*, *1977*, 129–143.

Rabbel, O., Galland, O., Mair, K., Lecomte, I., Senger, K., Spacapan, J. B., & Manceda, R. (2018). From field analogues to realistic seismic modelling: A case study of an oil-producing andesitic sill complex in the Neuquén Basin, Argentina. *Journal of the Geological Society*, *175*(4), 580–593. https://doi.org/10.1144/jgs2017-116

Reynolds, P., Planke, S., Millett, J., Jerram, D., Trulsvik, M., Schofield, N., & Myklebust, R. (2017). Hydrothermal vent complexes offshore Northeast Greenland: A potential role in driving the PETM. *Earth and Planetary Science Letters*, *467*, 72–78. https://doi.org/10.1016/j.epsl.2017.03.031

Roy, S., Senger, K., Hovland, M., Römer, M., & Braathen, A. (2019). Geological controls on shallow gas distribution and seafloor seepage in Arctic fjord of Spitsbergen, Norway. *Marine and Petroleum Geology*, *107*, 237–254. https://doi.org/10.1016/j.marpetgeo.2019.05.021

Saether, B., Johansen, S. E., Hesthammer, J., Solbakken, O., & Synnestvedt, K. (2004). Using geosimulators to enhance field-based geological training. *First Break*, *22*(6), 99–104. https://doi.org/10.3997/1365-2397.22.6.25901

Sartell, A. (2021). *The igneous complex of Ekmanfjorden, Svalbard: An integrated field, petrological and geochemical study*. Lund University.

Saumur, B., Dewing, K., & Williamson, M.-C. (2016). Architecture of the Canadian portion of the High Arctic Large Igneous Province and implications for magmatic Ni–Cu potential. *Canadian Journal of Earth Sciences*, *53*(5), 528–542. https://doi.org/10.1139/cjes-2015-0220

Schofield, N., Holford, S., Millett, J., Brown, D., Jolley, D., Passey, S., et al. (2015). Regional magma plumbing and emplacement mechanisms of the Faroe-Shetland Sill Complex: Implications for magma transport and petroleum systems within sedimentary basins. *Basin Research*, *29*(1), 41–63. https://doi.org/10.1111/bre.12164

Schröder-Adams, C. J., Herrle, J. O., Selby, D., Quesnel, A., & Froude, G. (2019). Influence of the High Arctic igneous province on the Cenomanian/Turonian boundary interval, Sverdrup Basin, high Canadian Arctic. *Earth and Planetary Science Letters*, *511*, 76–88. https://doi.org/10.1016/j.epsl.2019.01.023

Senger, K., Betlem, P., Birchall, T., Buckley, S. J., Coakley, B., Eide, C. H., et al. (2020). Using digital outcrops to make the high Arctic more accessible through the Svalbox database. *Journal of Geoscience Education*, 1–15.

Senger, K., Betlem, P., Birchall, T., Buckley, S. J., Coakley, B., Eide, C. H., et al. (2021). Using digital outcrops to make the High Arctic more accessible through the Svalbox database. *Journal of Geoscience Education*, *69*(2), 123–137. https://doi.org/10.1080/10899995.2020.1813865

Senger, K., Brugmans, P., Grundvåg, S.-A., Jochmann, M., Nøttvedt, A., Olaussen, S., et al. (2019). Petroleum exploration and research drilling onshore Svalbard: A historical perspective. *Norwegian Journal of Geology*, *99*(3), 1–30. https://doi.org/10.17850/njg99-3-1

Senger, K., Planke, S., Polteau, S., Ogata, K., & Svensen, H. (2014). Sill emplacement and contact metamorphism in a siliciclastic reservoir on Svalbard, Arctic Norway. *Norwegian Journal of Geology*, *94*, 155–169.

Senger, K., Roy, S., Braathen, A., Buckley, S. J., Bælum, K., Gernigon, L., et al. (2013). Geometries of doleritic intrusions in central Spitsbergen, Svalbard: An integrated study of an onshore-offshore magmatic province with implications on CO_2 sequestration. *Norwegian Journal of Geology*, *93*, 143–166.

Senger, K., Smyrak-Sikora, A., Kuckero, L., Rodes, N., & Betlem, P. (2022). Svalbard Rock Vault - Liberating vintage geoscience data from Svalbard (0.0.1) [Dataset]. Zenodo. https://doi.org/10.5281/zenodo.5919082

Senger, K., Tveranger, J., Braathen, A., Olaussen, S., Ogata, K., & Larsen, L. (2015). CO_2 storage resource estimates in unconventional reservoirs: Insights from a pilot-sized storage site in Svalbard, Arctic Norway. *Environmental Earth Sciences*, *73*(8), 3987–4009. https://doi.org/10.1007/s12665-014-3684-9

Senger, K., Tveranger, J., Ogata, K., Braathen, A., & Planke, S. (2014). Late Mesozoic magmatism in Svalbard: A review. *Earth-Science Reviews*, *139*, 123–144. https://doi.org/10.1016/j.earscirev.2014.09.002

Shephard, G., Trønnes, R., Spakman, W., Panet, I., & Gaina, C. (2016). Evidence for slab material under Greenland and links to Cretaceous High Arctic magmatism. *Geophysical Research Letters*, *43*(8), 3717–3726. https://doi.org/10.1002/2016gl068424

Shipilov, E., & Karyakin, Y. (2011). The Barents Sea magmatic province: Geological-geophysical evidence and new $^{40}Ar/^{39}Ar$ dates. *Doklady Earth Sciences*, *439*(1), 955–960. https://doi.org/10.1134/s1028334x11070270

Shkola, I. V. (1977). Processing results from parametric drill hole Grumant-1 in western Svalbard near Coles Bay (Report 5125, Leningrad) [Dataset]. PANGAEA. https://doi.org/10.1594/PANGAEA.688742

Shkola, I. V. (2007). Chemical composition of gabbro-dolerite from Hole Grumant-1 drilled in the West Svalbard. In I. V. Shkola (Ed.), (1977): *Processing results from parametric drill Hole Grumant-1 in western Svalbard near Coles Bay (Report 5125, Leningrad)*. All-Russian Research Institute for Geology and Mineral Resources of the World Ocean. https://doi.org/10.1594/PANGAEA.626560

Skilbrei, J. R. (1992). Preliminary interpretation of aeromagnetic data from Spitsbergen, Svalbard Archipelago (76°–79°N): Implications for structure of the basement. *Marine Geology*, *106*(1–2), 53–68. https://doi.org/10.1016/0025-3227(92)90054-l

Skjelkvåle, B.-L., Amundsen, H., O'Reilly, S. Y., Griffin, W., & Gjelsvik, T. (1989). A primitive alkali basaltic stratovolcano and associated eruptive centres, northwestern Spitsbergen: Volcanology and tectonic significance. *Journal of Volcanology and Geothermal Research*, *37*(1), 1–19. https://doi.org/10.1016/0377-0273(89)90110-8

Smelror, M., & Larssen, G. B. (2016). Are there Upper Cretaceous sedimentary rocks preserved on Sørkapp land, Svalbard? *Norwegian Journal of Geology*, *96*(2), 147–158. https://doi.org/10.7850/njg96-2-05

Smyrak-Sikora, A., Johannessen, E. P., Olaussen, S., Sandal, G., & Braathen, A. (2018). Sedimentary architecture during Carboniferous rift initiation–the arid Billefjorden Trough, Svalbard. *Journal of the Geological Society*, *176*(2), 225–252. https://doi.org/10.1144/jgs2018-100

Smyrak-Sikora, A., Nicolaisen, J. B., Braathen, A., Johannessen, E. P., Olaussen, S., & Stemmerik, L. (2021). Impact of growth faults on mixed siliciclastic-carbonate-evaporite deposits during rift climax and reorganisation—Billefjorden Trough, Svalbard, Norway. *Basin Research*, *33*(5), 2643–2674. https://doi.org/10.1111/bre.12578

Spacapan, J. B., Galland, O., Leanza, H. A., & Planke, S. (2016). Control of strike-slip fault on dyke emplacement and morphology. *Journal of the Geological Society*, *173*(4), 573–576. https://doi.org/10.1144/jgs2015-166

Spacapan, J. B., Palma, J. O., Galland, O., Manceda, R., Rocha, E., D'Odorico, A., & Leanza, H. A. (2018). Thermal impact of igneous sill-complexes on organic-rich formations and implications for petroleum systems: A case study in the northern Neuquén Basin, Argentina. *Marine and Petroleum Geology*, *91*, 519–531. https://doi.org/10.1016/j.marpetgeo.2018.01.018

Spacapan, J. B., Palma, O., Galland, O., Senger, K., Ruiz, R., Manceda, R., & Leanza, H. A. (2019). Low resistivity zones at contacts of igneous intrusions emplaced in organic-rich formations and their implications on fluid flow and petroleum systems: A case study in the northern Neuquén Basin, Argentina. *Basin Research*, *32*(1), 3–24. https://doi.org/10.1111/bre.12363

Steel, R. J., & Worsley, D. (1984). Svalbard's post-Caledonian strata—An atlas of sedimentational patterns and paleogeographic evolution. In A. M. Spencer (Ed.), *Petroleum geology of the north European Margin* (pp. 109–135). Graham & Trotman.

Svensen, H., Corfu, F., Polteau, S., Hammer, Ø., & Planke, S. (2012). Rapid magma emplacement in the Karoo large igneous province. *Earth and Planetary Science Letters*, *325–326*, 1–9. https://doi.org/10.1016/j.epsl.2012.01.015

Svensen, H., Jamtveit, B., Planke, S., & Chevallier, L. (2006). Structure and evolution of hydrothermal vent complexes in the Karoo Basin, South Africa. *Journal of the Geological Society*, *163*(4), 671–682. https://doi.org/10.1144/1144-764905-037

Svensen, H., Planke, S., Malthe-Sorenssen, A., Jamtveit, B., Myklebust, R., Rasmussen Eidem, T., & Rey, S. S. (2004). Release of methane from a volcanic basin as a mechanism for initial Eocene global warming. *Nature*, *429*(6991), 542–545. https://doi.org/10.1038/nature02566

Svensen, H., Planke, S., Polozov, A. G., Schmidbauer, N., Corfu, F., Podladchikov, Y. Y., & Jamtveit, B. (2009). Siberian gas venting and the end-Permian environmental crisis. *Earth and Planetary Science Letters*, *277*(3–4), 490–500. https://doi.org/10.1016/j.epsl.2008.11.015

Svensen, H. H., Jerram, D. A., Polozov, A. G., Planke, S., Neal, C. R., Augland, L. E., & Emeleus, H. C. (2019). Thinking about LIPs: A brief history of ideas in large igneous province research. *Tectonophysics*, *760*, 229–251. https://doi.org/10.1016/j.tecto.2018.12.008

Tarduno, J. (1998). The High Arctic Large Igneous Province. *Paper presented at Third International Conference on Arctic Margins* (pp. 12–16). Alfred Wegener Institute for Polar and Marine Research, the Federal.

Treiman, A. H. (2012). Eruption age of the Sverrefjellet volcano, Spitsbergen island, Norway. *Polar Research*, *31*(1), 17320. https://doi.org/10.3402/polar.v31i0.17320

Verba, M. L. (2015). Interaction of igneous and sedimentary rocks of archipelago of Svalbard in the light of the petroleum potential evaluation. *Neftegazovaya Geologiya Teoriya I Praktika*, *10*(4). https://doi.org/10.17353/2070-5379/46_2015

Wesenlund, F., Grundvåg, S.-A., Engelschiøn, V. S., Thieβen, O., & Pedersen, J. H. (2021). Linking facies variations, organic carbon richness and bulk bitumen content–a case study from the organic-rich Middle Triassic shales of eastern Svalbard. *Marine and Petroleum Geology*, *132*, 105168. https://doi.org/10.1016/j.marpetgeo.2021.105168

Westoby, M., Brasington, J., Glasser, N., Hambrey, M., & Reynolds, J. (2012). 'Structure-from-Motion' photogrammetry: A low-cost, effective tool for geoscience applications. *Geomorphology*, *179*, 300–314. https://doi.org/10.1016/j.geomorph.2012.08.021

Wilton, D. H., Saumur, B. M., Gordon, A., & Williamson, M.-C. (2019). Enigmatic massive sulphide mineralization in the High Arctic Large Igneous Province, Nunavut, Canada. *Canadian Journal of Earth Sciences*, *56*(7), 790–801. https://doi.org/10.1139/cjes-2018-0156

Worsley, D. (2008). The post-Caledonian development of Svalbard and the western Barents Sea. *Polar Research*, *27*(3), 298–317. https://doi.org/10.1111/j.1751-8369.2008.00085.x

Zuchuat, V., Sleveland, A., Twitchett, R., Svensen, H., Turner, H., Augland, L., et al. (2020). A new high-resolution stratigraphic and palaeoenvironmental record spanning the End-Permian Mass Extinction and its aftermath in central Spitsbergen, Svalbard. *Palaeogeography, Palaeoclimatology, Palaeoecology*, *554*, 109732. https://doi.org/10.1016/j.palaeo.2020.109732